






Cite this: *Green Chem.*, 2025, **27**, 4094

## Harnessing the potential of biphasic solvent systems in lignocellulosic biomass fractionation through computational insights†

Maryam Saleknezhad, <sup>a,b</sup> Meysam Madadi, <sup>\*a</sup> Salauddin Al Azad<sup>a</sup> and Vijai Kumar Gupta <sup>\*c,d</sup>

Biphasic solvent systems have emerged as a transformative approach for the efficient fractionation of lignocellulosic biomass (LCB), driving substantial progress in biofuel and biochemical production. By precisely partitioning lignin into the organic phase and hemicellulose into the aqueous phase while maintaining cellulose within the solid fraction, biphasic systems present a sophisticated and integrative strategy for LCB processing. This dual-phase approach achieves superior product separation and significantly enhances economic viability through the recyclability of solvents and catalysts. Several biphasic systems, including those employing 2-methyltetrahydrofuran, immiscible alcohol-based systems (butanol, pentanol, and phenoxyethanol), and ketones (Methyl isobutyl ketone), have been developed for LCB fractionation. Among these, immiscible alcohol-based systems have emerged as the most effective, demonstrating the ability to minimize cellulose degradation (1.0–30.0%) while optimizing the removal of hemicellulose (80.0–98.0%) and lignin (65.0–92.0%). The efficiency of these systems is largely due to strong hydrogen bonding interactions between the solvents–catalysts and xylan and lignin, which enhance effective extraction, as confirmed by mechanistic computational analyses. Other factors such as selective lignin dissolution, phase separation, low polarity, and energy-efficient recovery are also emphasized. This review indicates that immiscible alcohol-based methods achieve superior glucose yields following enzymatic hydrolysis (85.0–95.0%) at high solid loadings (10.0–13.0%). Sustainability assessments further emphasize the advantages of biphasic systems, predicting a reduced environmental footprint and improved economic feasibility relative to conventional methods. Integrating artificial intelligence techniques with these findings holds the potential to accelerate the industrial adoption of biphasic systems, optimizing process efficiency and reducing costs.

Received 24th November 2024,  
Accepted 25th February 2025

DOI: 10.1039/d4gc05977h

rsc.li/greenchem

### Green foundation

1. This review highlights the innovative application of biphasic solvent systems for the efficient fractionation of lignocellulosic biomass. It showcases their ability to separate key components—cellulose, hemicellulose, and lignin—while minimizing byproduct formation and enhancing economic viability through the use of recyclable solvents and catalysts. Furthermore, each separated component can be utilized in value-added bio-products.
2. The sustainable processing of lignocellulosic biomass is crucial for the development of biofuels and biochemicals, addressing global energy demands and environmental concerns. The advancements in biphasic systems represent a significant step towards achieving high conversion efficiencies, making this area of study relevant to a wide range of industries, including renewable energy and materials science.
3. The integration of artificial intelligence with biphasic solvent systems is expected to optimize process efficiencies and reduce costs, facilitating their industrial adoption. This review provides a comprehensive analysis of current methodologies and their sustainability assessments, guiding future research directions and promoting the development of greener technologies in the field.

<sup>a</sup>Key Laboratory of Industrial Biotechnology, Ministry of Education, School of Biotechnology, Jiangnan University, Wuxi 214122, China.

E-mail: m.madadi@jiangnan.edu.cn

<sup>b</sup>Department of Biotechnology, Faculty of Biological Science and Technology, University of Isfahan, Isfahan 81746-73441, Iran

<sup>c</sup>School of Biotechnology, Dublin City University, Glasnevin, Dublin, D09 K20V, Ireland. E-mail: vijaikumar.gupta@dcu.ie

<sup>d</sup>DCU Life Sciences Institute, Dublin City University, Dublin, D09 K20V, Ireland

† Electronic supplementary information (ESI) available. See DOI: <https://doi.org/10.1039/d4gc05977h>

## 1. Introduction

Dependence on fossil resources for energy and chemicals has driven a transition towards a bioeconomy focused on resource use efficiency and carbon reduction.<sup>1</sup> This transition aims to alleviate environmental concerns and achieve more sustainable metrics.<sup>2</sup> Lignocellulosic biomass (LCB) has emerged as a pivotal component in this transition due to its wide availability and annual production (~13 billion metric tonnes).<sup>2,3</sup> Utilizing LCB can significantly reduce reliance on fossil fuels, lower CO<sub>2</sub> emissions, and combat climate change.<sup>4</sup> Therefore, the efficient conversion of LCB into high-value products, including biofuels, biochemicals, and functional materials through biorefinery processes, offers a promising alternative to traditional fuels and chemicals. These advancements highlight the potential of biorefinery technologies to foster a sustainable, circular bioeconomy.<sup>5</sup> However, challenges remain, particularly in developing efficient pretreatment processes and addressing cost concerns to ensure economic viability.<sup>6</sup>

LCB, derived primarily from vascular plants, is composed of cellulose (30.0–50.0%), hemicellulose (15.0–30.0%), and lignin (10.0–30.0%).<sup>7</sup> Cellulose, a linear polysaccharide of glucose units, forms both crystalline and amorphous regions.<sup>8</sup> Hemicellulose, a branched carbohydrate, contains diverse polysaccharides and varies by LCB type.<sup>9</sup> Lignin, an amorphous polymer of aromatic monomers, provides structural strength and resistance to pathogens.<sup>10</sup> Typically, a pretreatment step is required to separate these components, breaking down lignin-carbohydrate complexes (LCCs), solubilizing hemicellulose, and disrupting cellulose's crystalline structure to increase surface area and facilitate enzymatic hydrolysis.<sup>11</sup> Over the past years, various pretreatment methods, including physical, chemical, and biological approaches, have been employed for different LCB fractionations.<sup>10,12</sup> The primary mechanism of LCB fraction-

ation, advantages, as well as disadvantages of these pretreatment methods are summarized in Table 1. For example, physical pretreatments, like grinding and milling, reduce particle size and increase surface area but are energy-intensive and costly.<sup>13</sup> Chemical pretreatments include acidic, alkaline, ionic liquid, deep eutectic solvents (DES), liquid hot water, and organosolv.<sup>14,15</sup> Among them, dilute acid hydrolysis effectively penetrates cell structures and breaks down hemicellulose structures.<sup>16</sup> Despite its cost-effectiveness, dilute acid pretreatment faces challenges with acid recovery and inhibitory byproducts like 5-hydroxymethylfurfural (HMF) and furfural (FF).<sup>2,17</sup> On the other hand, alkali pretreatment removes lignin and, partially, hemicellulose while preserving cellulose, enhancing its accessibility for subsequent processing.<sup>18</sup> However, it typically requires longer reaction times and generates black liquor, which demands costly post-treatment.<sup>19</sup> Additionally, salt deposition during the process can hinder downstream efficiency.<sup>20</sup> Furthermore, hemicellulose hydrolysis may result in sugar loss and the formation of inhibitory compounds (phenolics and furan).<sup>20,21</sup> Organosolv pretreatment targets lignin, depolymerizing it into soluble phenolic fragments with minimal inhibitory byproduct formation and efficient lignin recovery.<sup>22</sup> Various acids used under mild conditions co-remove lignin and hemicellulose, minimizing inhibitory byproducts and preventing lignin condensation.<sup>23</sup> Compared with acid and liquid hot water pretreatment, lignin from organosolv pretreatment undergoes fewer structural changes.<sup>24</sup> Solvent recycling and product recovery remain critical limitations of this method, and it suffers from reduced economic efficiency.<sup>25,26</sup>

The inefficiency and operational challenges in processing LCB have spurred the development of more efficient methods, such as biphasic solvent systems pretreatment.<sup>39</sup> This eco-friendly approach improves the recovery of dissolved lignin and hemicellulose, yielding purer products.<sup>40</sup> Biphasic pre-



**Maryam Saleknezhad**

*Maryam Saleknezhad obtained her MSc from Malek Ashtar University of Technology in 2020 and is currently pursuing a PhD in Chemical Engineering – Biotechnology at the University of Isfahan, Iran. Her research focuses on advanced pretreatment methods, enzymatic hydrolysis, and fermentation processes for efficient conversion of lignocellulosic biomass into biofuels and value-added biochemicals. She is particularly interested in*

*optimizing these processes to enhance yield, reduce costs, and improve sustainability in biorefinery applications.*



**Meysam Madadi**

*Meysam Madadi completed his PhD at Huazhong Agricultural University in 2021 and pursued his postdoctoral research at Jiangnan University in 2023. He is currently an Associate Professor at the Key Laboratory of Industrial Biotechnology, Jiangnan University. His research is primarily focused on innovative biorefinery strategies, biochemical engineering, bioenergy production, and the green synthesis of recyclable, value-added*

*products from lignocellulosic biomass. His work aims to advance sustainable bioeconomy solutions by optimizing resource efficiency and reducing environmental impact.*

**Table 1** The primary mechanism of action, advantages, and disadvantages of each method<sup>14,17,22,27–38</sup>

Pretreatment methods	The primary mechanism of action	Advantages	Disadvantages
Physical	Particle size reduction	Increasing porosity Improved access Simplicity	Incomplete disruption High energy consumption
Dilute acid	Protonation of the glycosidic oxygen Hemicellulose degradation	Effective in breaking down hemicellulose Enhancing the enzymatic digestibility of cellulose	Formation of inhibitors Generates acidic wastewater
Alkaline	Reduces cellulose degree of polymerization Depolymerize lignin Polymorphous lattice and CrI of cellulose	Effective in breaking down lignin Enhancing the enzymatic digestibility of cellulose Promoting the swelling process Shortening the dissolution time	High cost of the reactors and acid corrosion Loss of some hemicellulose Formation of inhibitors
Ionic liquid	Alters the structure of cellulose, dissolves cellulose, hemicellulose, and lignin, disrupting the crystalline structure of cellulose and increasing its accessibility	Highly effective in dissolving LCB and can be tuned to target specific biomass components Lower production of by-products	Expensive Difficult to recover and recycle Have a high negative environmental impact Inhibitory effects on the enzyme activity
DES	Fractionation of polymers Cellulose accessibility	Mild reaction conditions Efficient lignin removal Reduced sugar loss	High viscosity Some types have toxicity
Hydrothermal (liquid hot water, steam explosion)	Hydrolysis of hemicelluloses Fiber separation	Mild pretreatment Reducing expensive recovery costs No additional catalysts	Low lignin removal Energy-intensive Formation of inhibitors Low yield of fermentable sugars Formation of toxic compounds
Organosolv	Lignin removal Breaks the recalcitrance	Effective in separating lignin from carbohydrates The solvents used can be recovered and recycled Leaving behind cellulose that can be readily hydrolyzed	High capital investment and energy cost Cost of solvent recycling
Biological	Separating hemicellulose and lignin from cellulose Breakdown of complex biopolymers high enzyme with activity	Low-cost Environmentally friendly Doesn't produce toxic by-products	Slower process The low lignin removal Non-industrial

**Salauddin Al Azad**

*Salauddin Al Azad is currently pursuing his PhD at Jiangnan University. His research primarily focuses on biomass fractionation, molecular dynamics simulations, and density functional theory. His work aims to develop advanced techniques for efficiently utilising biomass and to explore the molecular mechanisms underlying biomass conversion processes, contributing to sustainable and innovative biorefinery solutions.*

**Vijai Kumar Gupta**

*Vijai Kumar Gupta has been an Associate Professor at the School of Biotechnology, Dublin City University (DCU), Ireland, since January 2024. Previously, he was a Senior Fellow and Group Leader at the Biorefining and Advanced Material Research Centre at SRUC, Edinburgh, UK. His research focuses on developing advanced bioprocess, microbial cell engineering and fermentation technologies to valorise available bioresources*

*for the production of value-added biochemicals, biopolymer-based composites, bioproducts and fuels, and their potential to address key challenges of agri-food-environmental importance.*

treatment utilizes organic and aqueous phases to selectively partition lignin into the organic phase due to its hydrophobic nature, while hemicellulose remains in the aqueous phase and cellulose in the solid phase.<sup>11</sup> This method offers several advantages: simplified separations, reduced product degradation, the potential for product concentration, improved downstream separations, lower energy consumption for solvent recycling, and enhanced biomass solubility (Fig. 1).<sup>11,41,42</sup> In addition, biphasic pretreatment paves the way for lignin-first techniques, maximizing the utilization of LCB. This promising method has been the focus of numerous successful studies on LCB fractionation and the production of value-added products.<sup>43–46</sup> The growing interest in biphasic pretreatment, as illustrated in Fig. 2, highlights the need for a comprehensive, statistically grounded review. This review serves as the foundation of the present study, aiming to consolidate current knowledge and drive further advancements in the field.

Typically, biphasic solvent systems are employed in two primary ways, immiscible (biphasic) and miscible (monopha-

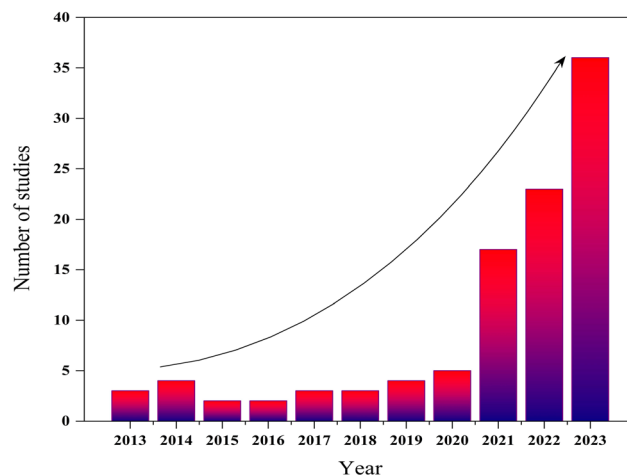


Fig. 2 The graph illustrates the increasing interest in biphasic pretreatment research. Data were obtained from Google Scholar searches using the following terms: "lignocellulose biphasic pretreatment", "biphasic solvent system", or "biphasic solvent fractionation".

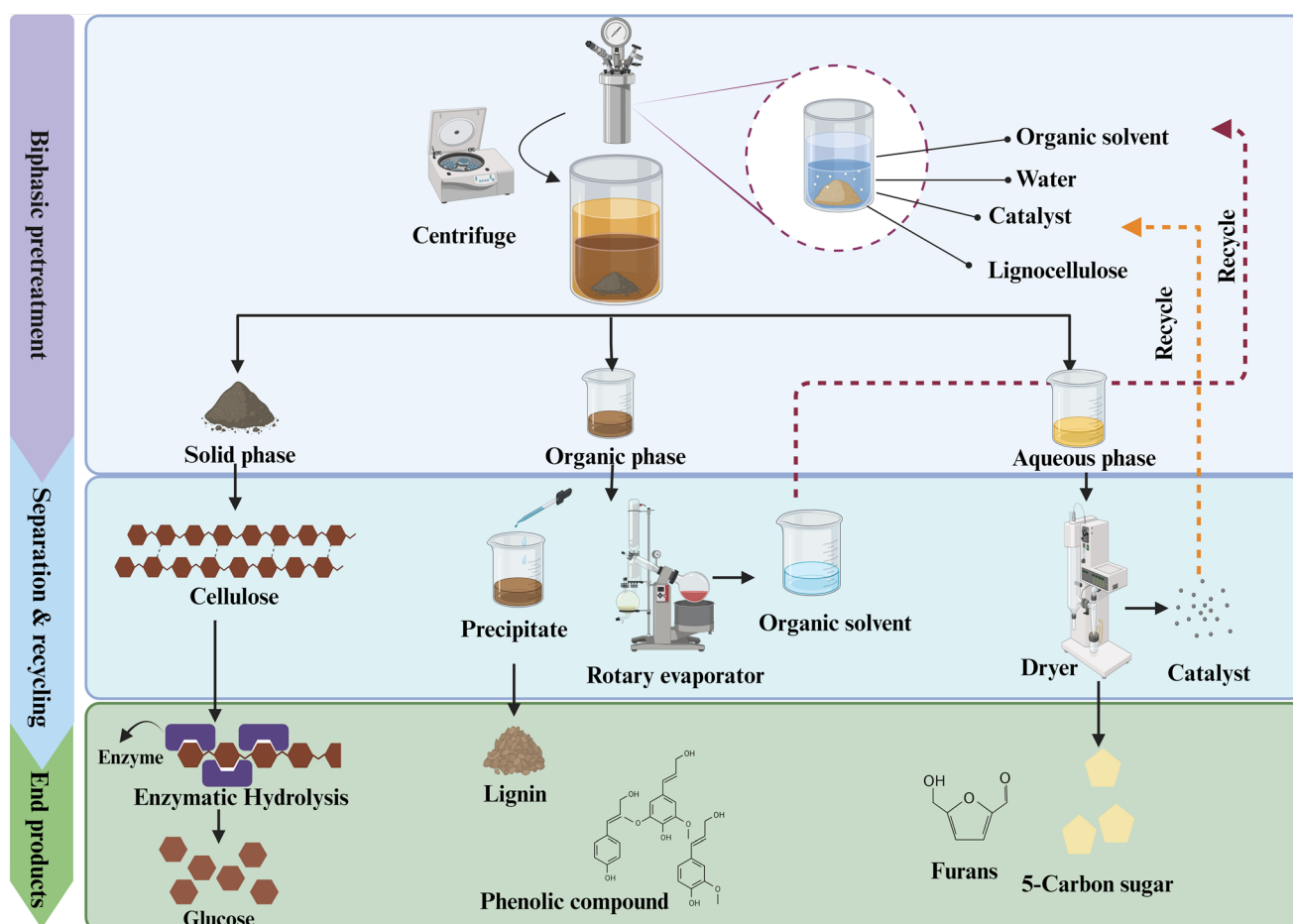
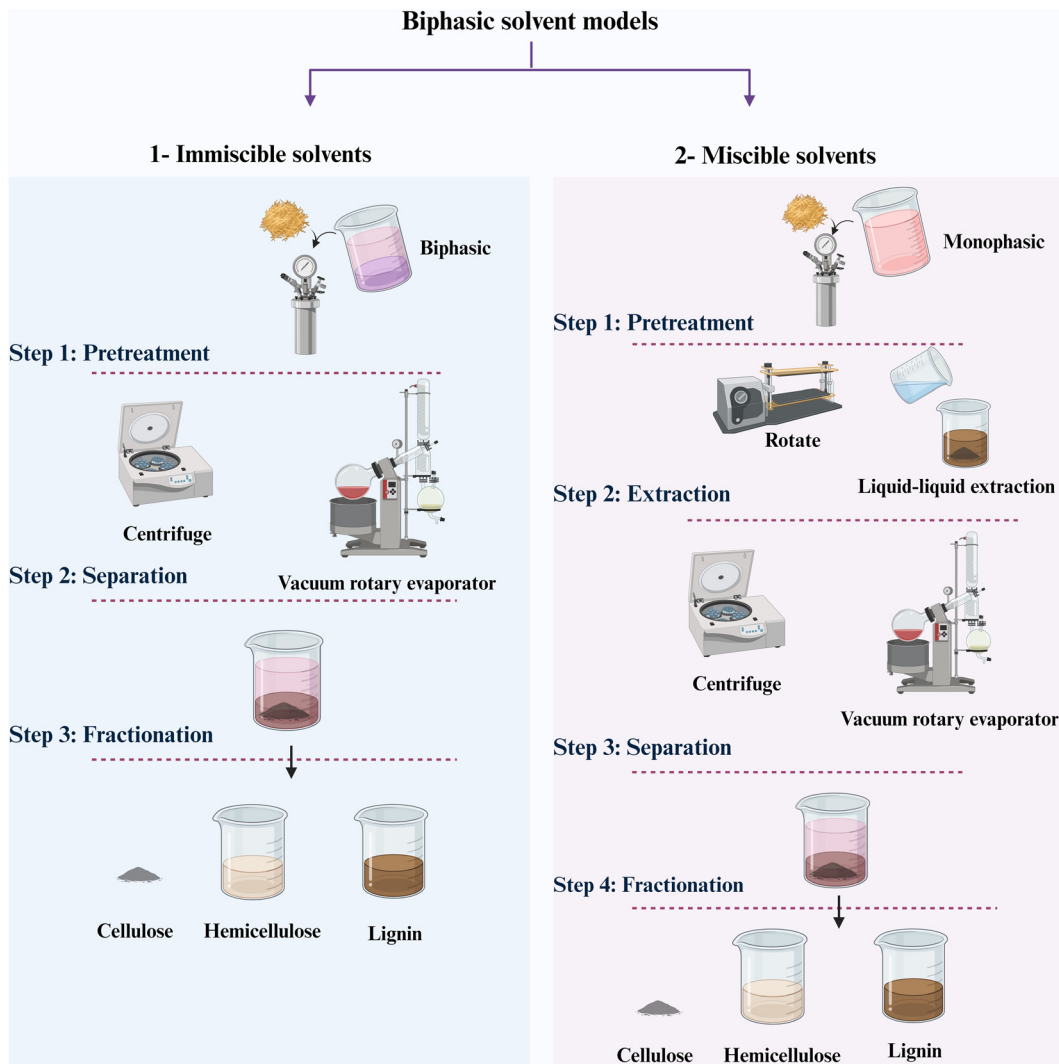


Fig. 1 This schematic depicts the fractionation process of LCB into various products through biphasic pretreatment. The pretreatment involves three steps: (i) LCB is treated with an organic solvent, catalyst, and water at a specific temperature and time. (ii) A centrifuge or funnel separates the pretreated mixture into three phases. (iii) The organic phase is concentrated by rotary evaporation. Certain catalysts may be recovered and recycled for reuse in precipitate pretreatment steps. The final products can be enriched in cellulose, glucose, lignin, phenolic compounds, furans, or 5-carbon sugars depending on the pretreatment goal.



**Fig. 3** This schematic illustrates two types of biphasic solvent systems used for LCB pretreatment: (1) immiscible solvents and (2) miscible solvents. LCB is pretreated with a mixture of two non-mixing solvents in the immiscible solvent system. After pretreatment, the mixture separates into two distinct liquid phases, which can be further processed. In the miscible solvent system, LCB is pretreated with a single, fully miscible solvent. Following pretreatment, a liquid–liquid extraction uses a second solvent to create two separate phases for product recovery.

sic) solvents (Fig. 3).<sup>40</sup> However, the phase state of a co-solvent in a liquid-phase reaction is determined by reaction temperature, pressure, the composition of the co-solvent system, resulting in either monophasic or biphasic systems.<sup>24</sup> The biphasic system consists of a reaction environment containing partially or fully immiscible aqueous and organic phases, commonly referred to as a classical biphasic system.<sup>42</sup> As the biomass reacts, solid cellulose precipitates, while the released sugars or furans remain in the aqueous layer, and lignin transfers into the organic phase.<sup>47</sup> This arrangement facilitates the enzymatic conversion of cellulose by reducing inhibitor concentrations in the aqueous phase.<sup>48</sup> In the second approach (non-classical), miscible solvents are initially used but later transition to a biphasic state through external triggers, such as the addition of salts (*e.g.*, through the salting-out effect) or solvents (*e.g.*, water). After this transition, a modifier is intro-

duced to establish a biphasic system that facilitates the separation of products using liquid-liquid extraction.<sup>49</sup> However, the 1-butanol/water system can exist in both monophasic and biphasic states. At temperatures above 120 °C, it forms a monophasic system, but upon cooling, it naturally transitions into a biphasic system without adding any modifier.<sup>24</sup> The classical biphasic system compared with the non-classical system leads to lower levels of FF and lignin precipitation on the cellulose surface.<sup>50</sup> These isolated components – hemicellulosic sugars, lignin, and cellulose – can then be further upgraded and converted into valuable bioproducts.<sup>51</sup> Even when monophasic systems are employed, processes can benefit from the biphasic system for product recovery.<sup>49</sup> Biphasic separations thus offer novel pathways for processing, requiring less energy for separations than monophasic systems due to solvent properties and reaction conditions.<sup>40,49</sup> The util-

ization of the biphasic system for LCB valorization is gaining popularity due to its superior advantages over its monophasic counterparts.<sup>40</sup> In these bifurcated systems, synthesized furans are optimally conserved as they rapidly transition to the organic phase upon formation, thereby mitigating side reactions.<sup>52</sup> Additionally, these reactions can be thermodynamically manipulated to favor the production of desired products, potentially lowering energy requirements for product recovery by enhancing furan yields and producing more concentrated products.<sup>52</sup> However, a gap exists in the current state-of-the-art: no comprehensive systematic review and assessment of the biphasic solvent fractionation and kinetic characteristics of LCB with different organic solvents throughout the separation process have been reported. Although ionic liquids can exhibit biphasic behavior in certain systems, they should not be confused with these biphasic solvent systems.

Fig. 4 presents a comprehensive timeline of significant advancements in biphasic pretreatment research. Initially, biphasic pretreatment emerged as a promising approach for suppressing humin formation and enhancing FF yield by selectively extracting it into an organic phase. This concept was pioneered by Trimble and Dunlop and expanded with solvents like Methyl isobutyl ketone (MIBK), as demonstrated by Dumesic's and Weingarten's work on fructose and xylose conversion, respectively.<sup>53–55</sup> A paradigm shift occurred in 2011 when vom Stein *et al.* introduced a biphasic system using methyl tetrahydrofuran (MeTHF) and oxalic acid (OA) to fractionate LCB into its primary components effectively. The ability to recover and reuse OA, coupled with the production of a cellulose-rich solid residue suitable for enzymatic hydrolysis, marked a significant breakthrough.<sup>7</sup> Building upon this, Liu *et al.* extended its application to FF production from pulp liquor.<sup>56</sup> The concept of industrial-scale biphasic pretreatment

was advanced by Viell *et al.* through the Organocat process. Their study compared it with traditional organosolv, highlighting potential economic and environmental advantages.<sup>57</sup> Characterization of lignin extracted using biphasic pretreatment by Calvaruso *et al.* revealed its potential for valorization into high-value chemicals.<sup>58</sup>

The development of pentanol-based biphasic pretreatment by Madadi *et al.* demonstrated high cellulose digestibility and lignin recovery while minimizing inhibitor formation and enabling efficient solvent recycling.<sup>43</sup> Moreover, Xie *et al.* employed computational modeling to elucidate the mechanisms underlying lignin depolymerization in various biphasic pretreatments, providing valuable insights for process optimization.<sup>59</sup> A landmark achievement was the 2024 study by Khounani *et al.*, which conducted the first comprehensive Life Cycle Assessment (LCA) of a pine chip-based biorefinery utilizing biphasic pretreatment.<sup>60</sup> By comparing the environmental impacts of biphasic pretreatment with conventional sulfuric acid pretreatment, the study offered critical insights into the sustainability of this technology.<sup>60</sup> This research significantly contributes to the development of environmentally benign and economically viable biorefinery processes.<sup>60</sup> Collectively, these advancements underscore the versatility and efficacy of biphasic pretreatment as a promising platform for unlocking the full potential of LCB. Continued research and development in this area are essential for advancing sustainable bio-based production of fuels, chemicals, and materials.

Based on the considerations and opportunities previously indicated, the recent advancements in biphasic pretreatment for LCB and their products underscore the value of a comprehensive review for both the scientific and industrial sectors. This review focuses on the classical biphasic solvent system and begins by evaluating the role played by different solvents

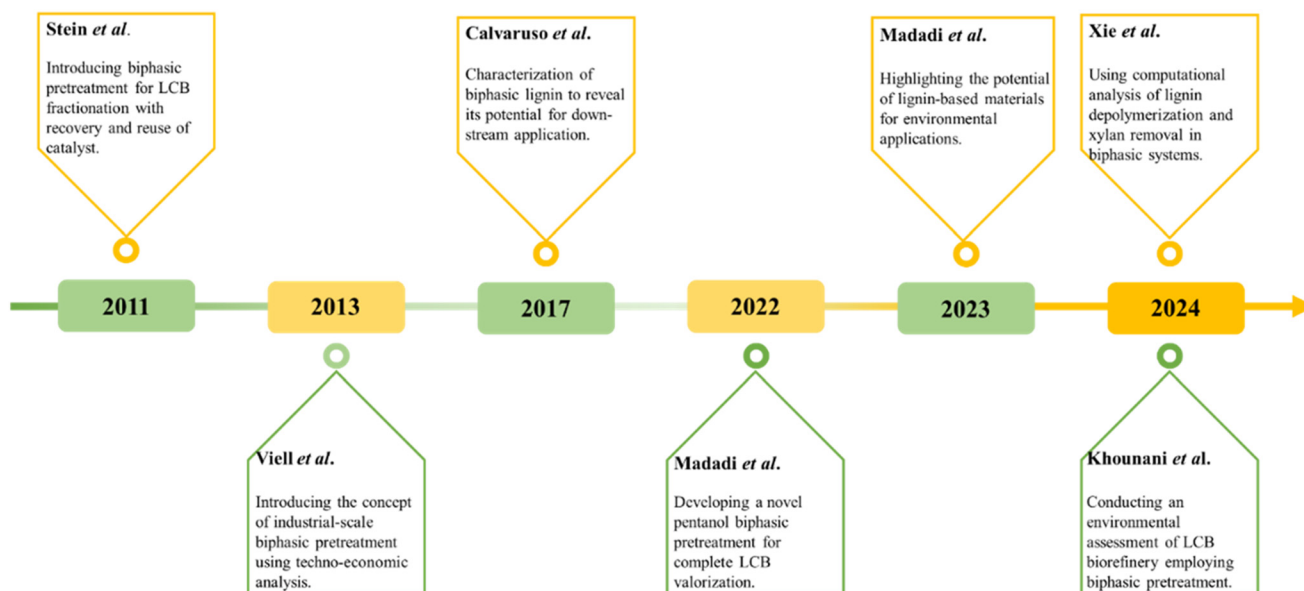


Fig. 4 Timeline of key milestones in the research and development of biphasic solvent systems for LCB pretreatment.

and catalysts in LCB fractionation, considering their properties. It then conducts a thorough analysis to understand how key parameters, such as solvent and catalyst types, along with time and temperature affect LCB fractionation. The fractionation mechanism is clarified through density functional theory (DFT) simulations. Furthermore, the review investigates the efficiency of biphasic-pretreated substrates on enzymatic hydrolysis and examines the impact of recovered solvent and catalyst on LCB fractionation and enzymatic hydrolysis. Additionally, it covers the recent progress in the LCA, techno-economic (TEA), and industrial-level assessments of biphasic solvent systems, promoting a circular bioeconomy and sustainability. By exploring these aspects, the review aims to identify opportunities to optimize biphasic pretreatment for efficient resource utilization and minimize environmental impact.

## 2. Solvent and catalyst in biphasic systems

Solvent selection in biphasic systems plays a critical role in impacting product yield, separation efficiency, and overall process sustainability.<sup>11</sup> Key considerations include solvent properties like flammability, viscosity, volatility, toxicity, and environmental impact.<sup>61</sup> Additionally, the polarity, basicity, and acidity of solvents are crucial.<sup>62</sup> In terms of polarity, high polarity facilitates cellulose dissolution by disrupting its crystalline structure and promoting sugar monomer formation, which preferentially partitions into the aqueous phase due to its high polarity.<sup>52,63</sup> In contrast, lignin and other non-polar organics exhibit different behavior, with branched molecules showing higher partition coefficients.<sup>64,65</sup> Optimal solvents demonstrate high polarity and basicity, influencing solute extraction capacity.<sup>11</sup> Apolar solvents often outperform polar ones in extracting furans and other non-polar organics from aqueous solutions, likely due to their ability to stabilize reactive intermediates through hydrogen bonding interactions.<sup>66</sup> Utilizing Hansen solubility parameters (HSP) in solvent selection can significantly enhance LCB processing efficiency,<sup>66</sup> enzymatic digestibility, and product yield, particularly in biphasic systems, as these systems can facilitate biochemical formation while minimizing degradation, improving overall process performance.<sup>55,67</sup>

Generally, two immiscible solvents typically rely on the catalyst to facilitate the transfer of reactants or intermediates between the aqueous and organic phases<sup>59,68</sup> and owe their efficacy to phase transfer catalysts.<sup>39</sup> This transfer mechanism significantly enhances reaction efficiency by promoting interactions at the interface of the two phases, thereby increasing the contact between reactants and accelerating reaction kinetics,<sup>22,52</sup> the driving force behind the advancement of sustainable biorefinery technologies.<sup>22,69</sup> Therefore, the choice of catalyst is equally critical in optimizing biphasic systems.<sup>11,42,70</sup> Catalyst modifications can be used to fine-tune biphasic systems, enabling the production of a wide range of high-value products,<sup>71</sup> or enabling efficient reaction processes

and reducing the formation of undesired products.<sup>72</sup> As a whole many catalysts significantly enhance the efficiency and effectiveness of biphasic systems used for LCB fractionation.<sup>73,74</sup>

The two types of homogeneous or heterogeneous catalysts utilized in biphasic systems each have unique advantages.<sup>49</sup> Homogeneous catalysts are preferred for their cost-effectiveness, miscibility, and high activity compared with their heterogeneous counterparts.<sup>52,75</sup> On the other hand, heterogeneous catalysts offer benefits in terms of easy recovery, tunability, and their effects on downstream reactions.<sup>52</sup> Categorizing these catalysts into homogeneous and heterogeneous types underscores their diverse yet complementary roles in optimizing LCB fractionation processes and advancing sustainable biorefinery technologies.<sup>40,74,76</sup>

Acid catalysts, for instance, play a crucial role in the hydrolysis of glycosidic bonds in hemicellulose, which promotes its dissolution in water by providing protons, and activating specific functional groups or facilitating essential reaction steps facilitating LCB fractionation processes and the formation of desired products.<sup>22,71,77</sup> OA and 2,5-furan dicarboxylic acid (FDCA) offer unique catalytic properties, promoting ester bond hydrolysis and potentially improving the efficiency of LCB fractionation within biphasic systems.<sup>42,78</sup> Studies show that OA can alter solvent properties, affecting polarity, acidity, and basicity.<sup>42,76</sup> Carboxylic acids, such as formic acid and acetic acid, act as homogeneous catalysts by promoting hydrolysis reactions of ester bonds within hemicellulose and lignin, thereby facilitating the solubilization or fragmentation of LCB components.<sup>79</sup> Similarly, sulfuric acid, another homogeneous catalyst, accelerates LCB degradation reactions and enhances the hydrolysis of glycosidic bonds in cellulose and hemicellulose.<sup>22,42</sup> The mentioned acids along with salts, such as sodium chloride and potassium chloride, serve as additional heterogeneous catalysts.<sup>77,80,81</sup> Conversely, Lewis acids, such as AlCl<sub>3</sub>, function as heterogeneous catalysts, expediting LCB breakdown through depolymerization and hydrolysis, thereby improving the solubilization or fragmentation of lignin and hemicellulose.<sup>71,82</sup>

In Fig. 5–9(A<sub>2</sub>, B<sub>2</sub> and C<sub>2</sub>), the most commonly used catalysts in fractionation within the reviewed biphasic systems are highlighted for their effects on LCB fractionation. The biphasic alcohol-based systems primarily utilize sulfuric acid, with a few studies employing *p*-TsOH. In contrast, the biphasic ether-based systems predominantly involve acids such as Lewis acids, sulfuric acid, carboxylic acids, FDCA, and OA. Additionally, Lewis acids and sulfuric acid are applied in biphasic ketone-based systems.

### 2.1. Biphasic solvent

This section highlights the most commonly employed solvents in different biphasic solvent systems, specifically focusing on LCB fractionation as the organic phase. The studied solvents include ethers, alcohols, and ketones, with their properties detailed in Table 2.

**2.1.1. MeTHF.** MeTHF, classified as a polar aprotic solvent, exhibits some polarity due to its oxygen atom but lacks acidic

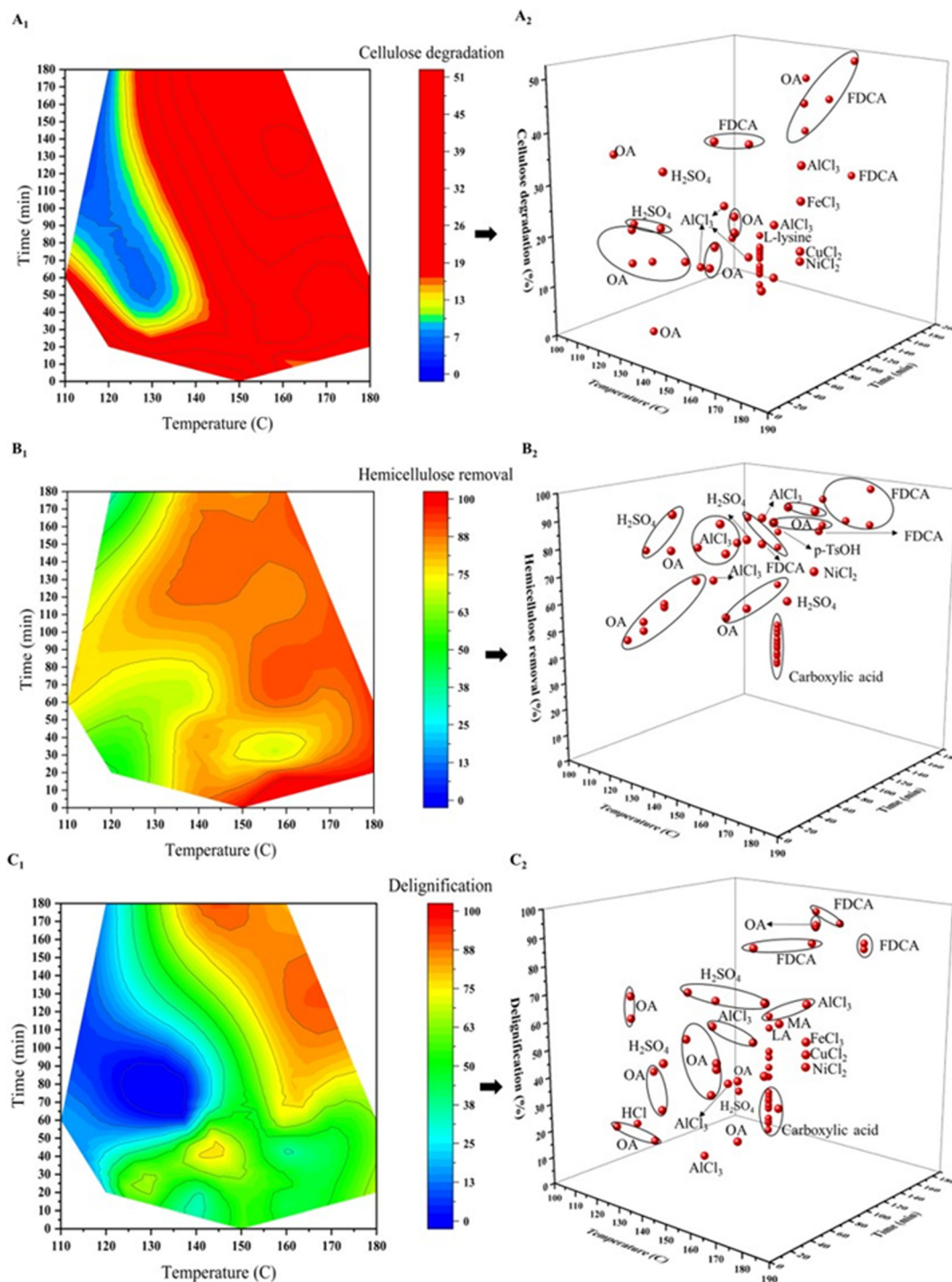


**Fig. 5** Profiling of biphasic pretreatment with MeTHF as an organic solvent. (A) Cellulose degradation (%), (B) hemicellulose removal (%), and (C) delignification (%). The data in the contour plots and 3D scatter are based on the literature review summarized in Table S1.†

hydrogens, making it a suitable medium for a wide range of reactions.<sup>68</sup> While generally stable under typical conditions, its reactivity can be influenced by specific reagents or catalysts. This property complements its emergence as a promising eco-friendly alternative among organic solvents.<sup>85</sup> Its limited miscibility with water and stability in acidic environments make it particularly attractive for specific applications.<sup>75,86</sup> As a cyclic

ether with an oxygen heterocyclic structure, MeTHF demonstrates high efficacy in extracting and fractionating LCB.<sup>87</sup> However, the effectiveness of this process hinges on the presence of a catalyst that can provide protons to break down the LCB complex, highlighting the crucial interplay between solvent and catalyst selection.<sup>42</sup> Furthermore, MeTHF possesses a favorable RED (1.3) parameter, contributing to its

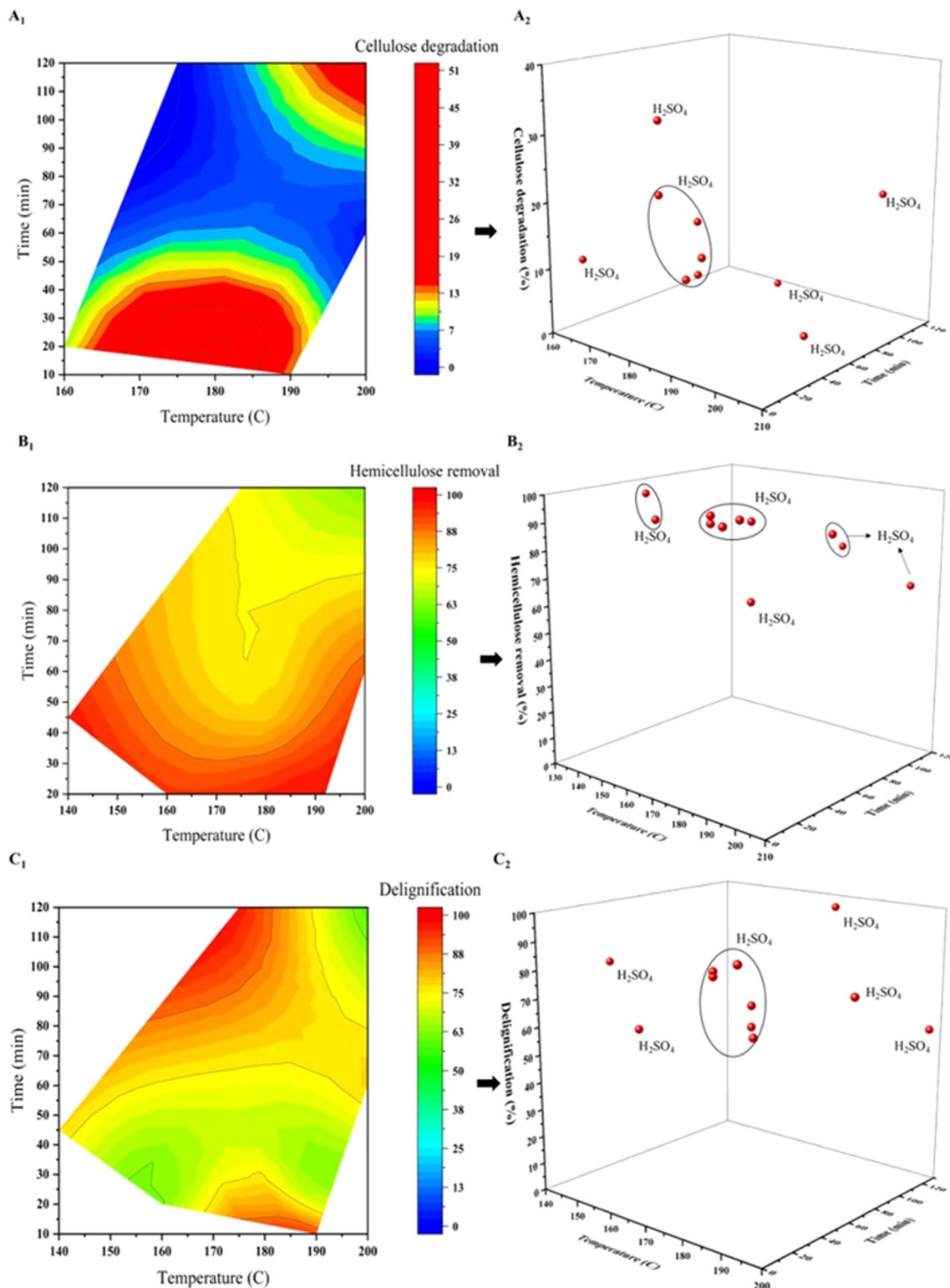


**Fig. 6** Profiling of biphasic pretreatment with butanol as an organic solvent. (A) Cellulose degradation (%), (B) hemicellulose removal (%), and (C) delignification (%). The contour plots and 3D scatter data are based on the literature review summarized in Table S1.†

interaction with lignin.<sup>86,87</sup> Its low boiling point (80.8 °C) further enhances its practical application, facilitating easy recycling after treatment.<sup>84</sup>

Studies on MeTHF as the organic phase in biphasic systems have identified  $\text{CuCl}_2$ ,  $\text{NiCl}_2$ ,  $\text{H}_2\text{SO}_4$ ,  $\text{FeCl}_3$ , FDCA,  $\text{AlCl}_3$ , and OA as popular catalysts (Table S1†).<sup>78,82,88</sup> Among

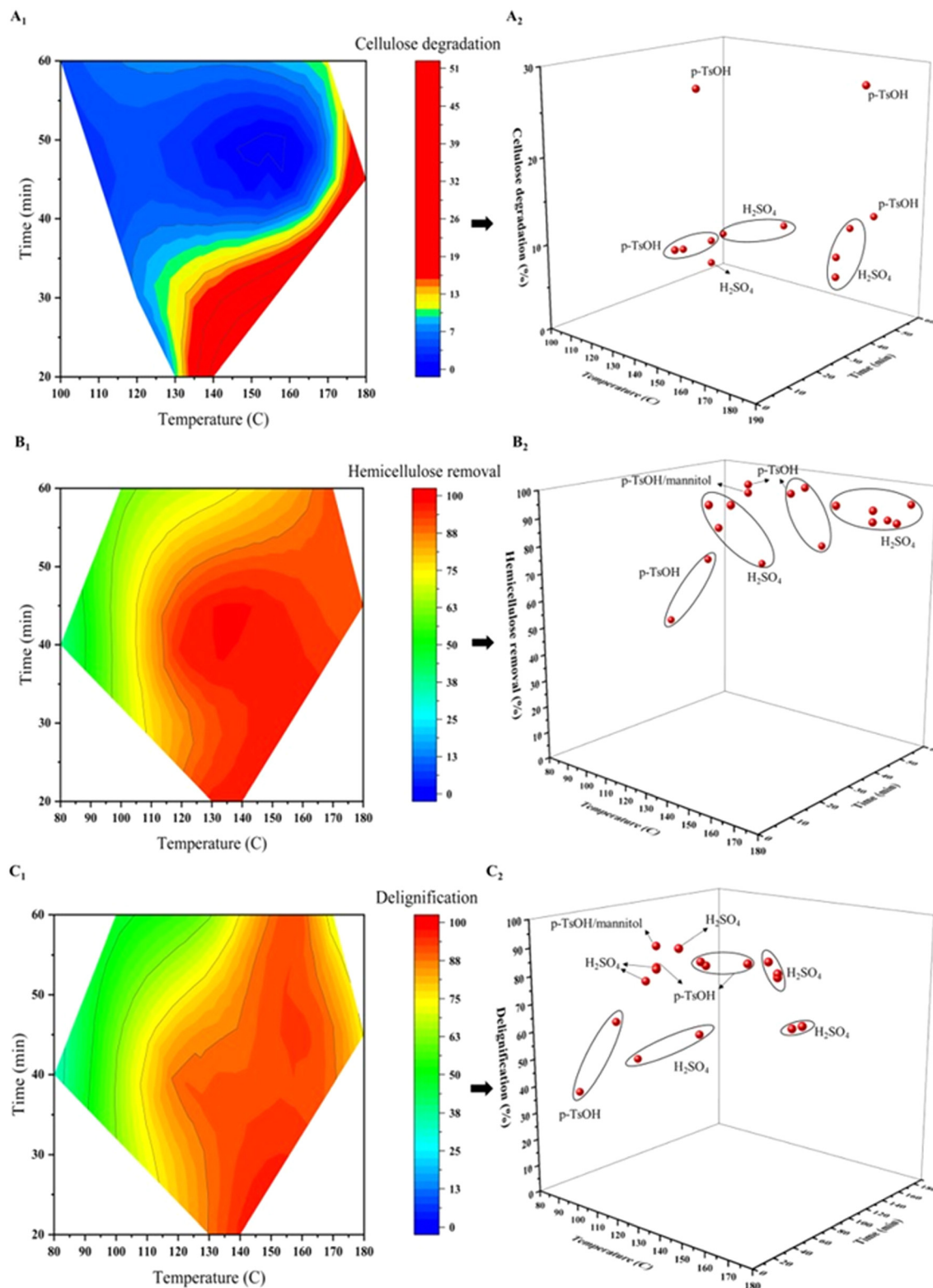


**Fig. 7** Profiling of biphasic pretreatment with pentanol as an organic solvent. (A) Cellulose degradation (%), (B) hemicellulose removal (%), and (C) delignification (%). The data in the contour plots and 3D scatter are based on the literature review summarized in Table S1.†

these, OA has received the most attention, particularly as an organocatalyst known as Organocat.<sup>87,89</sup> This catalyst induces physical and chemical alterations in LCB, including

size reduction, cell wall rupture, and elimination of fibrillar structures, indicating structural breakdown after pretreatment.<sup>90</sup> The removal of lignin, hemicellulose, and other

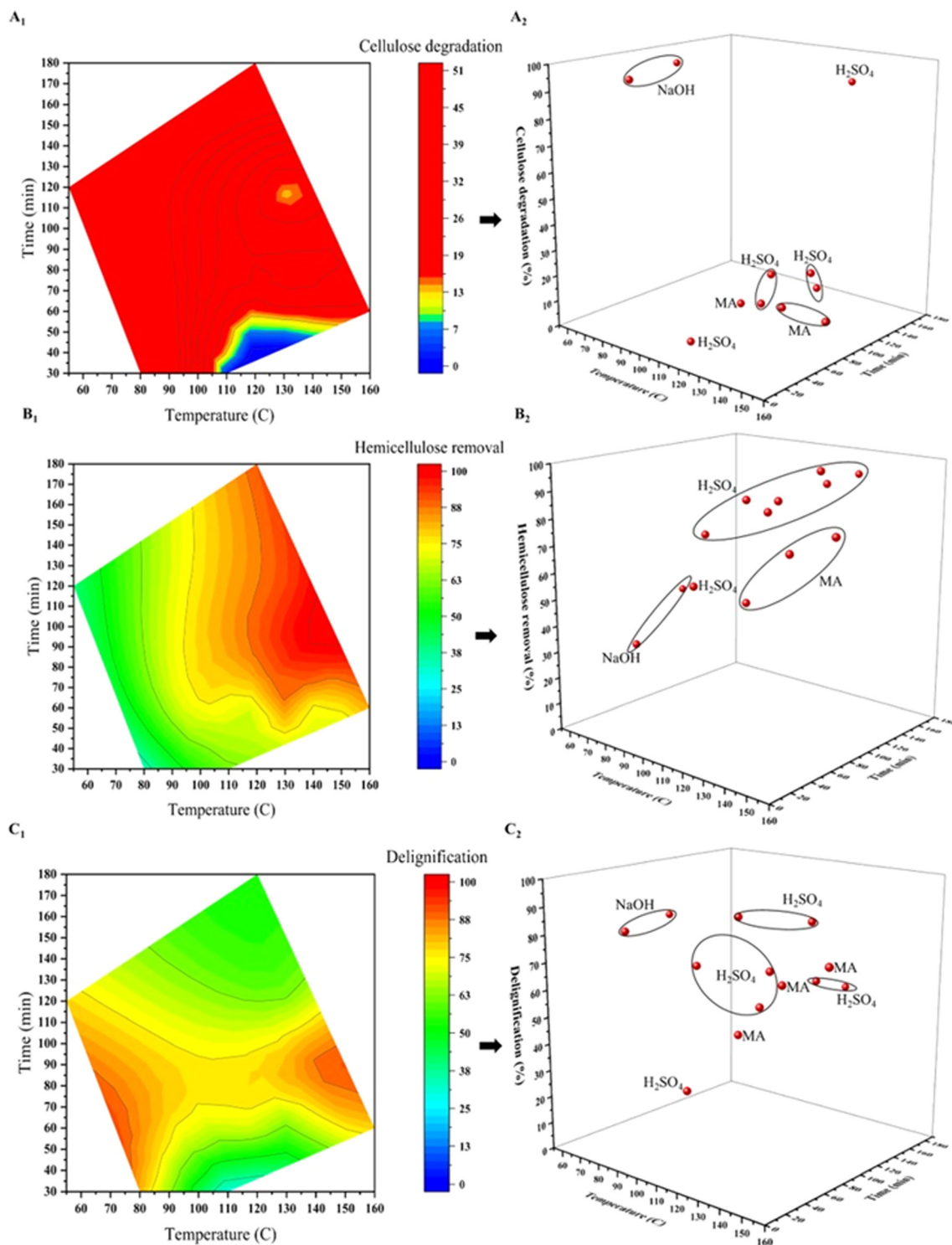


**Fig. 8** Profiling of biphasic pretreatment with phenoxyethanol as organic solvent. (A) Cellulose degradation (%), (B) hemicellulose removal (%), and (C) delignification (%). The data in the contour plots and 3D scatter are based on the literature review summarized in Table S1.†

extractives leads to pore formation, facilitating the segregation of cellulose fibers and effective depolymerization of LCB components under mild conditions.<sup>90,91</sup> This process enhances saccharification efficiency by improving enzyme accessibility to cellulose.<sup>87</sup>

Furthermore, OA can be separated and recycled within the system through precipitation. The process generates by-products such as organic acids and furan aldehydes, necessitating post-pretreatment steps involving the concentration of the aqueous fraction through water evaporation and subsequent cooling to

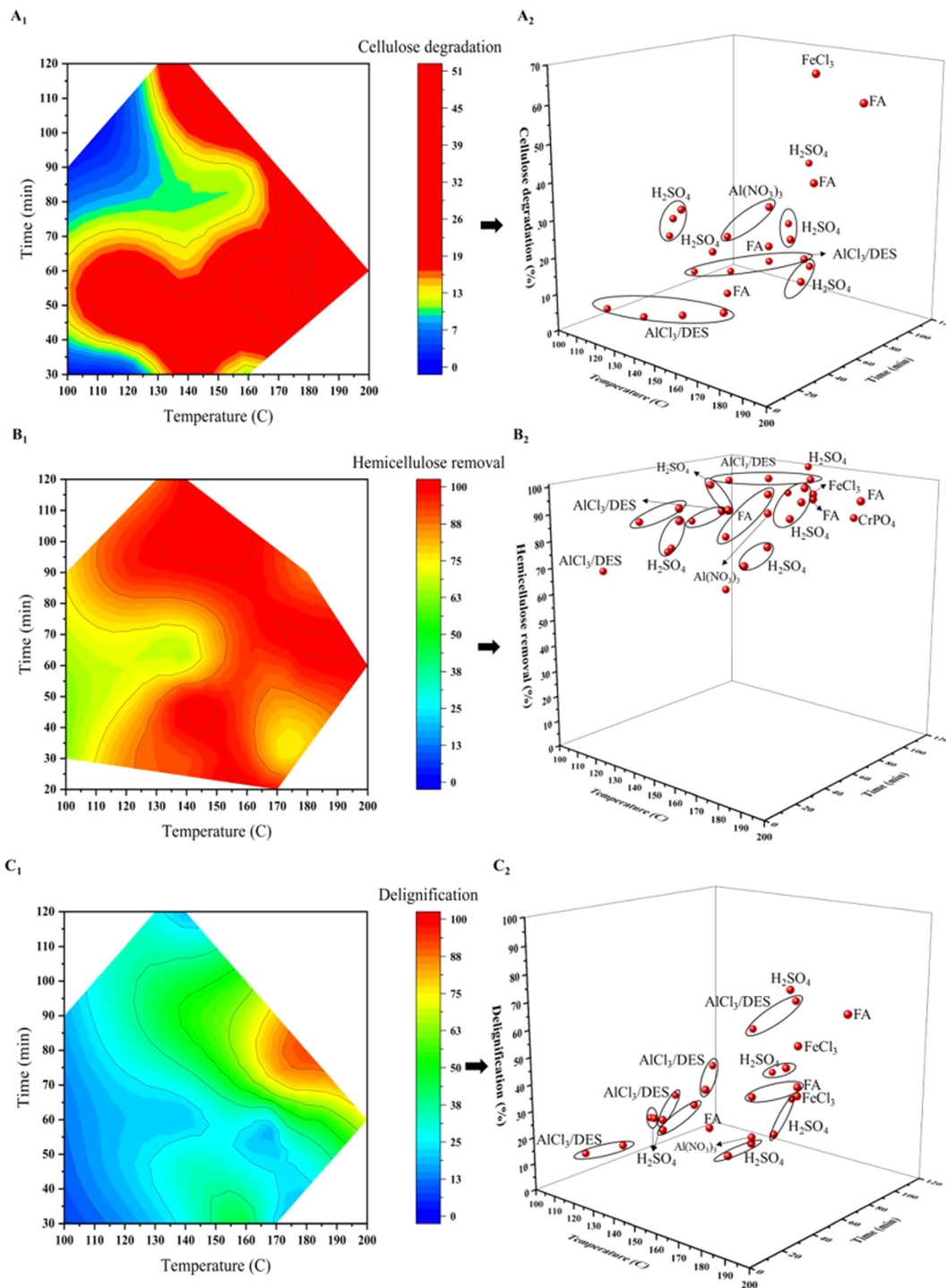


**Fig. 9** Profiling of biphasic pretreatment with MIBK as an organic solvent. (A) Cellulose degradation (%), (B) hemicellulose removal (%), and (C) delignification (%). The data in the contour plots and 3D scatter are based on the literature review summarized in Table S1.†

obtain OA crystals.<sup>89</sup> Filtration to remove the solid pulp enables the separation of the water and organic phases without product separation in repetitive batch mode, significantly enhancing biomass-to-catalyst and biomass-to-solvent ratios.<sup>22</sup> Additionally, the process yields lignin as a high-value intermediate, while liquid sugars can be directly converted into high-

value chemicals or biofuels, enhancing the economic viability of the entire process.<sup>42</sup> The combination of MeTHF with an OA catalyst shows promise, allowing for up to four reuse cycles.<sup>90</sup>

Both organic and mineral acids facilitate LCB fractionation by enabling proton-mediated cleavage of ether/ester bonds in LCCs.<sup>82</sup> In contrast, Lewis acids promote LCB fractionation by

**Table 2** Physical properties, solubility parameters, relative energy difference parameter (solvent–lignin) of organic solvent (MeTHF, 1-butanol, pentanol, phenoxyethanol, MIBK)

Solvent	Classification	Boiling point (°C)	Flash point (20 °C)	Vapor pressure (kPa)	Solubility in water <sup>a</sup> (g per 100 g)	RED <sup>b</sup>
MeTHF	Ether	80.8	−11.0	13.5	14.0	1.3
1-Butanol	Mono alcohol	117.7	29.0	0.6	7.7	1.0
Pentanol	Mono alcohol	137.9	43.0	0.6	2.2	1.1
Phenoxyethanol	Ether alcohol	245.0	127.0	0.0013	2.7	1.7
MIBK	Ketone	117.0	14.0	2.1	1.9	1.4

<sup>a</sup> Extracted from the International Chemical Safety Cards (ICSCs) database.<sup>83</sup> <sup>b</sup> The Relative Energy Difference (RED) is a dimensionless parameter derived from the HSP. It is calculated between lignin and a solvent within the three-dimensional solubility parameter space defined by dispersion ( $\delta_D$ ), polar ( $\delta_P$ ), and hydrogen-bonding ( $\delta_H$ ) forces.<sup>84</sup>

providing active protons to break linkages and disrupting hydrogen bonding networks in LCCs.<sup>59,82,92</sup> Besides Lewis acids, NaCl is often employed to offer chloride ions, aiding in the breakdown of hydrogen bonding in xylo-oligomers and enhancing the interaction between hydronium ions ( $H^+$ ) and xylo-oligomers, thereby accelerating hemicellulose solubilization accordingly.<sup>81,92</sup> However, adding NaCl or using more extreme reaction conditions promotes the conversion of xylose into FF, which could react with lignin to generate humins. These humins can redeposit on cellulose, thereby decreasing lignin removal efficiency.<sup>80,82</sup>

In the MeTHF system, FDCA emerges as a catalyst of significant interest, ranking as the third most studied (Table S1†). Renowned for its thermostability, weak acidity, and low ionization constant, FDCA's properties play a crucial role in its performance.<sup>43,78</sup> These attributes result in fewer  $H^+$ , which are critical for breaking down glycosidic bonds but can also lead to cellulose degradation at high concentrations.<sup>42</sup> FDCA's moderate acidity, crucial for selective cleavage of glycosidic bonds, particularly in hemicellulose and lignin, might require further optimization for even greater selectivity.<sup>78</sup> The release of  $H^+$  from FDCA can be amplified by increasing the pretreatment temperature, often necessitating harsh conditions (high temperature and extended duration).<sup>42</sup> This approach allows for the solubilization of hemicellulose and lignin but comes at the cost of higher energy consumption. While FDCA offers advantages like thermostability and selectivity, its economic feasibility requires further consideration, especially compared with established mineral acids ( $H_2SO_4$ , HCl) that are commonly used for LCB fractionation, although they may have drawbacks such as environmental impact and catalyst recovery challenges.<sup>85,93–95</sup>

### 2.1.2. Mono alcohols and ether alcohol

**2.1.2.1. 1-Butanol.** Mono alcohols have been utilized as organosolv agents in LCB pretreatments, attracting attention due to their favorable boiling points and recyclability.<sup>96</sup> Utilizing low-miscible alcohols in biphasic systems has facilitated constructive LCB fractionation.<sup>97</sup> 1-Butanol, characterized by its suitable boiling point and relative miscibility, derived from sustainable feedstocks, has been extensively studied (Table 2).<sup>70</sup> The results indicate that 1-butanol exhibits significant LCB breakdown capabilities compared with other

alcohols, attributed to its suitable boiling point, a more favorable Hansen number for lignin dissolution, and an acceptable RED parameter.<sup>11,84</sup> A study explored the use of a 1-butanol/water system for biomass fractionation under both monophasic and biphasic conditions, revealing that the biphasic system demonstrated superior effectiveness for pretreatment. This enhanced performance was primarily due to the system's selective solubility and phase separation capabilities, which enabled the efficient removal of lignin and hemicellulose. Under biphasic conditions, lignin was preferentially solubilized in the 1-butanol phase, while hemicellulose remained in the aqueous phase. This separation effectively prevented lignin repolymerization—a frequent challenge encountered in monophasic systems. Additionally, the 1-butanol/water system's ability to transition between monophasic and biphasic states, depending on thermodynamic conditions, offered a flexible and tunable approach for optimizing pretreatment efficiency.<sup>24</sup> Biphasic pretreatment with  $H_2SO_4$  offers a potential solution to catalyst inhibition. However, the strong Brønsted acidity of  $H_2SO_4$  can lead to unwanted side reactions.<sup>11</sup> Therefore, optimizing this system requires balancing  $H_2SO_4$ 's effectiveness with maximizing LCB fractionation. Research shows that using OA and 1-butanol, compared with MeTHF, leads to higher efficiency in LCB breakdown and subsequent production of fermentable sugars after hydrolysis.<sup>98</sup> These results suggest that 1-butanol can act as a good solvent for catalyst interaction and facilitate efficient LCB fractionation during pretreatment. Additionally, an attractive feature of this approach is the potential for a closed-loop system where the 1-butanol solvent is a product of the fermentation process itself.<sup>98</sup>

**2.1.2.2. Pentanol.** The unique properties of alcohols make them indispensable for inefficient biomass processing, as they penetrate the LCB structure and disrupt the LCCs.<sup>63,99</sup> These attributes render alcohol invaluable in the pretreatment of LCB.<sup>100</sup> Research indicates that alcohols with lower miscibility in water, such as pentanol, are preferred for fractionation (Table 2).<sup>22</sup> The strategic use of these solvents in pretreatment is to enhance enzyme accessibility to cellulose.<sup>70</sup> Pentanol, characterized by its low water solubility and optimal boiling temperature, effectively removes lignin and hemicellulose, the primary components of the protective matrix surrounding cellulose fibers.<sup>43</sup> This removal process not only preserves the

polymeric integrity of cellulose by reducing hydrolysis but also renders it more amenable to subsequent enzymatic hydrolysis.<sup>70</sup> Recent research highlights pentanol as a promising solvent for lignin removal.<sup>43,101,102</sup> Utilizing a mixture of pentanol and an acid catalyst for fractionation offers significant energy savings compared with conventional ethanol-based methods and facilitates straightforward solvent separation *via* rotary vacuum evaporation.<sup>43</sup> This approach enables high cellulose recovery rates and demonstrates efficient cleavage of ester and ether linkages in lignin, as well as glycosidic bonds in hemicelluloses.<sup>41,43</sup>

Traditionally, H<sub>2</sub>SO<sub>4</sub> has been the catalyst of choice.<sup>43</sup> However, recent studies suggest substituting *p*-toluenesulfonic acid (*p*-TsOH) due to its stability, recyclability,<sup>44</sup> and lower boiling point. *p*-TsOH exhibits excellent proton-donating capabilities in solvents, promoting efficient lignin and hemicellulose solubilization under mild pretreatment conditions.<sup>42</sup> Operational parameters play a crucial role in determining the properties of the extracted lignin. Higher water proportions result in lignin fractions lacking aliphatic β-O-4 units, while increased pentanol content preserves a substantial portion of native β-O-4 linkages.<sup>40,41,43</sup> Despite the potential of pentanol-soluble lignin as a biomaterial source due to its low contaminant sugar levels and high phenolic hydroxyl group content, harsher treatments may lead to undesired lignin repolymerization.<sup>44</sup>

**2.1.2.3. Phenoxyethanol.** Phenoxyethanol, recognized for its green and non-toxic properties, offers a sustainable solution for lignin extraction.<sup>66,103</sup> As a biocompatible and biodegradable organic solvent, it exhibits near-complete immiscibility with water, making it a promising candidate for a two-phase solvent pretreatment system (Table 2).<sup>104</sup> The solubility of lignin in alcohols is highest in phenoxyethanol, outperforming 1-butanol and pentanol, suggesting its effectiveness for lignin extraction and recovery. Its potency is further enhanced when combined with acid and alkaline catalysts.<sup>105</sup> Acid catalysts, for instance, provide protons that expedite the hydrolysis of glycosidic linkages within hemicellulose, enhancing its solubility in water.<sup>42</sup>

### 2.1.3. Ketone

**2.1.3.1. MIBK.** Owing to its distinctive properties, MIBK stands out as a preferred solvent in the biphasic system for LCB fractionation. Notably, its low miscibility with water ensures the formation of a separate organic phase, which is essential for the efficient separation and purification of biomass components (Table 2).<sup>106</sup> MIBK's ability to effectively dissolve lignin and FF helps prevent furan degradation and increases yield.<sup>107,108</sup> Additionally, the moderate boiling point of MIBK facilitates solvent recovery and recycling, thereby enhancing the economic viability of industrial applications.<sup>23</sup> Using catalysts like H<sub>2</sub>SO<sub>4</sub> and AlCl<sub>3</sub> plays a pivotal role in enhancing productivity. Studies have shown that H<sub>2</sub>SO<sub>4</sub> degrades a significant amount of cellulose and produces high levels of FF, while FeCl<sub>3</sub> also yields high hemicellulose removal.<sup>105,109,110</sup> However, using catalysts other than H<sub>2</sub>SO<sub>4</sub> may lead to FF degradation at elevated temperatures.<sup>11,14</sup>

## 2.2. Biphasic solvent system-specific pretreatment for lignocellulosic biomass fractionation

Recent studies have investigated various solvents and catalytic conditions at different temperatures and durations to optimize LCB fractionation, considering delignification, xylan removal, cellulose degradation, and enzymatic conversion rates. This section presents a comparative analysis of the relative operation conditions (*i.e.*, temperature, duration, solvent variety, and catalyst type) and provides a visual summary, and highlights the distribution of fractionation efficiency. In biphasic pretreatment, a range of solvents has been explored, including ethers (MeTHF), alcohols (1-butanol, pentanol, and phenoxyethanol), and ketones (MIBK), as detailed in Table S1.† Fig. 5–9 present a statistical and comparative analysis of each solvent's performance, considering catalyst type, reaction time, and temperature. These analyses were conducted using Origin Pro version 2024 software.

The figures employ 3D scatterplot modeling to visualize the effects of various conditions (catalyst, time, temperature) on cellulose degradation (%) (A), hemicellulose removal (%) (B), and delignification (%) (C) achieved by the different solvents (data referenced from Table S1†). The contour plot on the left-hand side of each figure illustrates the rate of cellulose degradation as a function of temperature (*X*-axis) and time (*Y*-axis). The color gradient, transitioning from blue to red, represents a spectrum from minimal to substantial degradation.

**2.2.1. MeTHF-based pretreatment.** Fig. 5 presents the profiling of a biphasic pretreatment process utilizing MeTHF solvent. Fig. 5A<sub>1</sub> reveals a relationship between temperature and time with cellulose degradation. A rightward shift in the contour lines with increasing temperature indicates that higher temperatures promote more pronounced degradation. Additionally, extended durations at elevated temperatures result in greater cellulose degradation exceeding 15.0%. Fig. 5A<sub>2</sub> provides further detail by highlighting the impact of different catalysts on cellulose degradation. The results suggest a significant influence of catalysts on both temperature and pretreatment time. OA catalysts, while promising, demonstrate variable performance based on time and temperature. At milder temperatures and shorter durations, OA catalysts lead to approximately 15.0% cellulose degradation.<sup>79,90</sup> Interestingly, low-temperature applications with homogeneous carboxylic acid catalysts show promising results.<sup>79</sup> Conversely, Lewis acids (AlCl<sub>3</sub>, FeCl<sub>3</sub>) and FDCA promote high levels of cellulose degradation even with brief treatment times.<sup>78,79,88</sup> By analyzing both plots, suitable operating conditions for minimizing cellulose degradation can be identified. For instance, the model suggests that using the OA catalyst within a temperature range of 120–140 °C for a maximum duration of 100 minutes could potentially achieve cellulose degradation below 15.0%.

Fig. 5B<sub>1–2</sub> explore the impact of time, temperature, and catalyst selection on hemicellulose removal. Fig. 5B<sub>2</sub> highlights the effectiveness of various catalysts, including AlCl<sub>3</sub>, OA, FDCA, and H<sub>2</sub>SO<sub>4</sub>. FDCA appears to be particularly successful in

achieving higher hemicellulose removal. While Fig. 5B<sub>1</sub> shows that high temperatures over a wide range of durations can facilitate effective 5-carbon sugar release, severe conditions may lead to the production of furans and the degradation of sugars. This necessitates adjustments in the severity of the conditions for optimal fractionation. Modeling suggests that a brief duration (60–80 minutes) at high temperatures within the 160–180 °C range may be optimal for achieving higher hemicellulose removal while minimizing cellulose degradation.

Fig. 5C<sub>1</sub> analyzes the effectiveness of different catalysts in delignification. OA and FDCA outperform H<sub>2</sub>SO<sub>4</sub>, carboxylic acids, and Lewis acids in this aspect. Fig. 5C<sub>1</sub> illustrates that at temperatures above 160 °C, delignification levels exceeding 80.0% can be achieved within 70 to 90 minutes. However, the analysis suggests a trade-off. While MeTHF shows promise in achieving high removal for hemicellulose and lignin (Fig. 5B and C), it requires prolonged operation times. Moreover, high temperatures increase the risk of inhibitor production and lignin loss.

By analyzing the combined information from Fig. 5 the model can identify suitable operating conditions for minimizing cellulose degradation while maximizing hemicellulose removal and delignification during the MeTHF pretreatment process. Therefore, for optimal performance, process conditions of 170–180 °C for 70–90 minutes are recommended for this solvent, with FDCA serving as the catalyst.

**2.2.2. 1-Butanol-based pretreatment.** Research on 1-butanol pretreatment currently lacks extensive data on the impact of various catalysts. While H<sub>2</sub>SO<sub>4</sub> remains the most frequently reported, its effectiveness heavily depends on operating conditions. Fig. 6A<sub>1</sub> illustrates cellulose degradation across various temperatures (160–190 °C) and operation times. Unfortunately, these conditions often exceed the desired threshold of less than 15% cellulose degradation. Modeling suggests a potential compromise that utilizing a lower temperature (160 °C) for up to 60 minutes might minimize cellulose degradation while still achieving some degree of fractionation. Fig. 6A<sub>2</sub> highlights the dependence of cellulose degradation on operating conditions. It reveals that H<sub>2</sub>SO<sub>4</sub> can degrade cellulose by up to nearly 35.0%, depending on time and temperature. This emphasizes the importance of selecting appropriate catalysts and optimizing operating conditions to minimize cellulose loss during fractionation. Fortunately, while cellulose degradation needs management in 1-butanol pretreatment, this system allows for high percentages of hemicellulose removal within a short duration (>1 h). Fig. 6B<sub>2</sub> demonstrates that this solvent system, with H<sub>2</sub>SO<sub>4</sub>, has a high potential for substantial hemicellulose removal across a wide range of times and temperatures. In contrast, significant delignification occurs with different time–temperature combinations in the 1-butanol system (Fig. 6C), extended operation times (70 to 120 minutes) at lower temperatures (160–170 °C), and short operation times (>30 minutes) at higher temperatures (180–190 °C). This flexibility allows researchers to tailor the process to their specific goals for hemicellulose removal and

delignification. Based on modeling results from Fig. 6, a pretreatment condition of 180 °C for up to 45 minutes with H<sub>2</sub>SO<sub>4</sub> as the catalyst is recommended for 1-butanol pretreatment. This finding offers valuable guidance for achieving high levels of hemicellulose removal and delignification while controlling cellulose degradation. Further research may explore the impact of different catalysts on achieving optimal fractionation in 1-butanol pretreatment.

**2.2.3. Pentanol-based pretreatment.** Fig. 7 explores pentanol pretreatment with *p*-TsOH and H<sub>2</sub>SO<sub>4</sub> catalysts. Fig. 7A<sub>1</sub> suggests that mild temperatures (>130 °C) for up to 60 minutes can minimize cellulose degradation, whereas higher temperatures increase the degradation rate. Analyzing Fig. 7A<sub>2</sub> reveals that *p*-TsOH, depending on time and temperature, results in varying degrees of cellulose degradation. Conversely, H<sub>2</sub>SO<sub>4</sub> degrades cellulose to less than 15%. Both *p*-TsOH and H<sub>2</sub>SO<sub>4</sub> achieve high hemicellulose removal exceeding 80% (Fig. 7B<sub>2</sub>). Fig. 7B<sub>1</sub> indicates that temperatures ranging from 130 °C to 160 °C within 50 minutes provide optimal conditions for hemicellulose removal (Fig. 7B<sub>1</sub>). The effectiveness of this catalyst system in delignification depends on time and temperature, with *p*-TsOH typically achieving higher delignification according to Fig. 7C<sub>2</sub>. Temperature has a more significant influence than time on delignification (Fig. 7C<sub>1</sub>). Overall, modeling suggests temperatures between 130 °C and 160 °C lead to high delignification. In contrast, pentanol exhibits minimal damage to cellulose. Additionally, pentanol demonstrates high levels of hemicellulose removal and delignification, nearing 100% under temperatures below 160 °C within 1 h. Based on modeling, the recommended operational conditions for the pentanol system are a temperature of 140 °C for 35 minutes with H<sub>2</sub>SO<sub>4</sub> as the catalyst.

**2.2.4. Phenoxyethanol-based pretreatment.** Phenoxyethanol solvent demonstrates promise for LCB fractionation due to its ability to achieve high hemicellulose removal while minimizing cellulose degradation. This is particularly evident with H<sub>2</sub>SO<sub>4</sub> as the catalyst. Fig. 8A<sub>1–2</sub> illustrates the significant impact of catalyst and operation condition type on the cellulose degradation rate. Among the tested catalysts (H<sub>2</sub>SO<sub>4</sub>, Maleic acid (MA), and NaOH), H<sub>2</sub>SO<sub>4</sub> exhibits the most desirable behavior, achieving cellulose degradation within the acceptable limit within 50 minutes at temperatures ranging from 110 to 140 °C. As shown in Fig. 8B<sub>2</sub> the effectiveness of H<sub>2</sub>SO<sub>4</sub> extends to hemicellulose removal and facilitates near-complete hemicellulose removal (~100%) at temperatures between 130 to 160 °C and within a time range of 60 to 100 minutes (Fig. 8B<sub>1</sub>). According to Fig. 8C<sub>2</sub>, H<sub>2</sub>SO<sub>4</sub> also exhibits superior delignification compared with other catalysts. Fig. 8C<sub>1</sub> further suggests that optimal delignification occurs at higher temperatures (140 to 160 °C) within 60 to 100 minutes. A key advantage of using phenoxyethanol is achieving high hemicellulose removal at temperatures >160 °C, minimizing cellulose degradation despite substantial delignification. H<sub>2</sub>SO<sub>4</sub> emerges as the most effective catalyst in this system, promoting an optimal environment for fractionation. Based on these findings, the recommended optimum conditions are a

temperature of 140 °C for 85 minutes using H<sub>2</sub>SO<sub>4</sub> as the catalyst.

**2.2.5. MIBK-based pretreatment.** Compared with the previous solvent, MIBK generally necessitates higher temperatures for effective LCB fractionation (Fig. 9). While Lewis acids and formic acid can achieve high cellulose degradation (>50.0%) under specific conditions (Fig. 9A<sub>2</sub>), their performance can be inconsistent. Conversely, H<sub>2</sub>SO<sub>4</sub> demonstrates superior consistency, with degradation rates ranging from 10.0% to 30.0%. Notably, the broader temperature range observed in Fig. 9A<sub>1</sub> suggests that acceptable cellulose degradation can be attained within a shorter timeframe (40 minutes) at moderate temperatures (100–130 °C). Fig. 9B<sub>1</sub> reveals two key strategies for maximizing hemicellulose removal, either employing lower temperatures (120–140 °C) for extended durations (80–100 minutes) or utilizing higher temperatures (140–190 °C) for shorter treatment times (40–60 minutes). H<sub>2</sub>SO<sub>4</sub> emerges as the most effective catalyst for achieving high hemicellulose removal (>90.0%), outperforming Lewis acids (Fig. 9B<sub>2</sub>). According to Fig. 9C<sub>2</sub>, while H<sub>2</sub>SO<sub>4</sub> is a powerful catalyst, MIBK exhibits limitations in achieving high delignification (maximum 75.0%). Fig. 9C<sub>1</sub> highlights this limitation through the red area, indicating that high temperatures (170–190 °C) for extended times (70–80 minutes) promote the degradation of other components, hindering effective delignification. The MIBK system offers a distinct advantage, including minimal cellulose degradation while achieving high hemicellulose removal. Catalysts like AlCl<sub>3</sub>, H<sub>2</sub>SO<sub>4</sub>, and FeCl<sub>3</sub> are particularly effective for hemicellulose removal. However, delignification remains a challenge within this system, as evidenced by modeling analysis. Although using H<sub>2</sub>SO<sub>4</sub> at 170 °C for 60 minutes might achieve both high hemicellulose removal and delignification, it comes at the cost of potentially increased cellulose degradation. Therefore, careful optimization is crucial when employing MIBK for LCB fractionation.

The LCB utilized in the biphasic systems is presented in Table S1.† They are categorized into hardwood, softwood, and agricultural residues. The most commonly utilized LCB in biphasic systems is agricultural residues, followed by hardwood (Fig. 10). Therefore, the suggested optimum reaction conditions could validate the use of these types of LCB. In biphasic ether-based systems, agricultural residues are predominant, followed by hardwood. In contrast, agricultural residues are the most studied in biphasic alcoholic-based systems (such as butanol and phenoxyethanol). However, in the pentanol and MIBK systems, hardwood materials are the most investigated (>50%).

### 3. Mechanism of fractionation in biphasic solvent systems

The mechanism of the biphasic solvent system involves the utilization of immiscible solvents and water under high temperature and pressure, which can affect the process in two significant ways. The interplay between Relative Energy Density

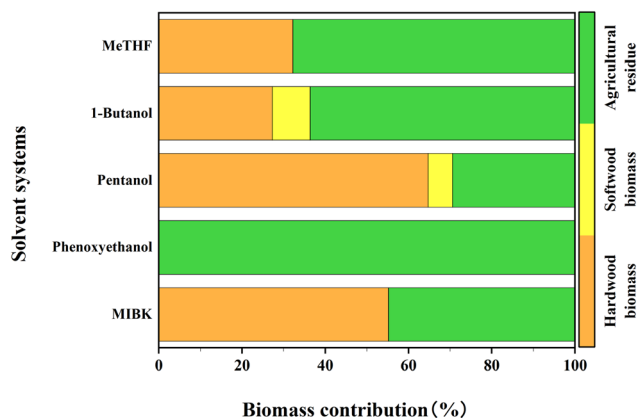


**Fig. 10** The most studied LCB material and scattering of softwood, hardwood, and agricultural in the biphasic solvent system. Based on the literature review summarized in Table S1.†

(RED) and Hansen solubility parameters is crucial for understanding the solubility and reactivity of lignin in various chemical processes. By leveraging these concepts, researchers can enhance lignin's utility in sustainable materials and energy applications. Specifically, selecting suitable immiscible solvents in a biphasic system can enhance the cleavage of lignin due to its high solubility at elevated temperatures. This situation allows for the transfer of lignin to the organic solvent while preventing precipitation on cellulose, thus facilitating the breakdown of cellulose into phenolic compounds in the hydrolysate. Moreover, transferring lignin to the organic phase and separating it from the system can yield near-pure lignin for advanced applications.

The interaction between lignin and the solvent primarily involves hydrogen bonding and dispersion forces, with solvents interacting with the hydroxyl groups present in lignin to facilitate its dissolution. Following significant delignification, hemicellulose can break down in water at elevated temperatures. The interaction between water and hemicellulose is significantly influenced by temperature and time, with hydrogen bonding being the primary mechanism driving solubility, while van der Waals forces and ionic interactions play supportive roles.

Although biphasic solvents are typically applied with solvents that have higher boiling points than water, fractionation can be conducted under moderate conditions to prevent the formation of inhibitors. By controlling the conditions and solvent choice, the formation of undesirable byproducts can be minimized. Consequently, under mild conditions and without the presence of fragmented lignin, cellulose degradation remains low, allowing for a higher rate of transfer to monomers. In this system, the utilized catalyst plays a crucial role in hydrolyzing glycosidic bonds in hemicellulose, promoting its dissolution in water by providing protons and activating specific functional groups. This facilitation enhances the essential reaction steps involved in LCB fractionation processes, leading to improved depolymerization and hydrolysis,

thereby enhancing the solubilization and fragmentation of both lignin and hemicellulose.

### 3.1. Mechanism of fractionation in biphasic solvent systems *via* computational analysis

To gain insights into hemicellulose removal and delignification during the biphasic solvent systems process, computational analysis was conducted. Five systems, namely MeTHF/FDCA, 1-butanol/H<sub>2</sub>SO<sub>4</sub>, pentanol/H<sub>2</sub>SO<sub>4</sub>, phenoxyethanol/H<sub>2</sub>SO<sub>4</sub>, and MIBK/H<sub>2</sub>SO<sub>4</sub>, were selected for simulation with lignin (VG, veratrylglycerol-beta-guaiacyl ether) and xylan models due to their higher efficiency in LCB fractionation. VG was chosen as a lignin model because of its aromatic ring with methoxy (-OCH<sub>3</sub>) and hydroxyl (-OH) groups, featuring the β-O-4 interunit bonds.<sup>111</sup> The D-xylan model was used because it represents the hemicellulose component, which is crucial for understanding the solubilization and removal processes during pretreatment.<sup>59,112</sup>

**3.1.1. Density functional theory analysis of energy *via* molecular dynamics simulation.** In this analysis, the evaluation of the highest occupied molecular orbital (HOMO)–lowest unoccupied molecular orbital (LUMO) band gap was conducted to identify potential interaction sites in solvents and catalysts with VG and D-xylan.<sup>59,113</sup> The study of the HOMO–LUMO gap in quantum mechanics considers various parameters, including molecular structure (atomic composition, bond lengths, angles, and geometry), electronic configuration (electron distribution in molecular orbitals,

HOMO and LUMO occupation), and quantum mechanical properties (orbital energies, wave functions, and electron density).<sup>114,115</sup>

Based on the HOMO–LUMO analysis, H<sub>2</sub>SO<sub>4</sub> and FDCA emerged with the most favorable energy conditions, indicated by their lowest HOMO–LUMO gaps of 0.172 eV and 0.689 eV, respectively. This narrow gap suggests that these two catalysts, particularly H<sub>2</sub>SO<sub>4</sub>, are more chemically reactive, with better electrical conductivity and stability when combined with another solvent (Fig. 11). The HOMO–LUMO gap is a key determinant of a molecule's ability to donate or accept electrons, thereby influencing its chemical reactivity and energy profile.<sup>115</sup> In the context of LCB pretreatment, a smaller HOMO–LUMO gap, such as that observed with H<sub>2</sub>SO<sub>4</sub>, indicates a lower energy requirement for electron transfer processes. This characteristic can enhance the efficiency of solvent molecules in facilitating LCB fractionation.<sup>59</sup> The combination of MIBK with H<sub>2</sub>SO<sub>4</sub> achieved a HOMO–LUMO gap of 0.314 eV, followed by 1-butanol/H<sub>2</sub>SO<sub>4</sub> (1.435 eV), phenoxyethanol/H<sub>2</sub>SO<sub>4</sub> (2.565 eV), MeTHF/FDCA (2.565 eV), and pentanol/H<sub>2</sub>SO<sub>4</sub> (4.059 eV) (Fig. 11). This indicates that H<sub>2</sub>SO<sub>4</sub>-based systems may be more effective in LCB fractionation processes due to their favorable energy profiles.

**3.1.2. Electrostatic energy between biphasic solvent systems and lignin or xylan.** Performing Self-Consistent Field (SCF) calculations in quantum chemistry is fundamental for accurately determining the electronic structure of molecules,

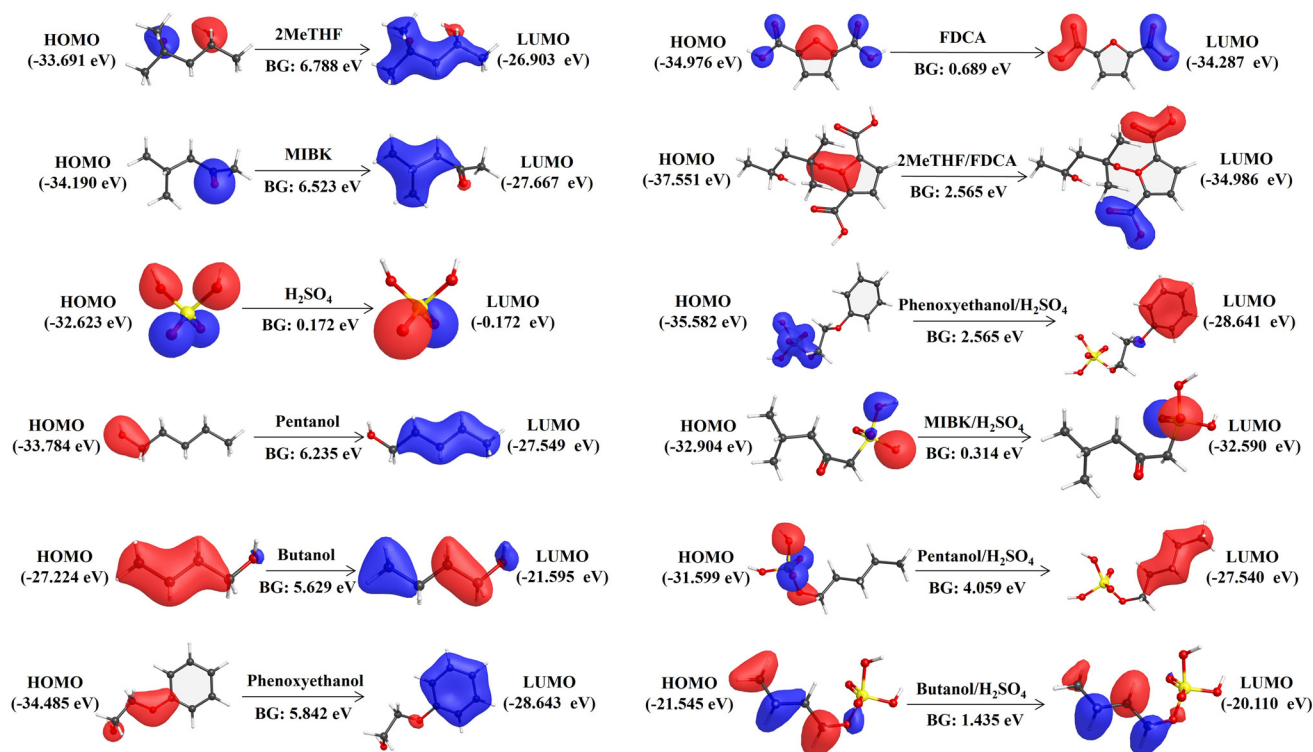


Fig. 11 Individual and combined energy density profiling of the chemical components based on their HOMO and LUMO energy band gaps.

crucial in assessing the HOMO–LUMO gap, which dictates reactivity and energy transfer capabilities.<sup>116</sup> SCF methods iteratively solve the electronic Schrödinger equation to achieve a self-consistent solution, providing precise molecular orbitals and energies.<sup>113,116</sup> The electrostatic energy and Reduced Density Gradient (RDG) are elucidated through SCF calculations by evaluating the interaction energies between molecular fragments or the gradient of electron density, respectively, providing insights into molecular interactions critical for understanding solvent–catalyst interactions in LCB conversion processes.<sup>59</sup> In this study, we concurrently discuss the distribution of SCF-based electrostatic energy on atomic surfaces and the RDG matrix, illustrated in Fig. 12. Electrostatic energy is visually represented with blue, indicating regions of high hydrogen (H) bonding density, correlating with elevated energy density. Conversely, reddish areas denote hydrogen-repulsive energy, indicative of lower energy

density.<sup>59,117</sup> These electrostatic surfaces qualitatively delineate both the higher and lower energy density aspects of individual and conjugated chemical structures. H-bonding plays a crucial role in the separation process of lignin and xylan, as it governs the solubility and interaction of LCB components with solvents, facilitating their dissolution and extraction. Strong H-bonding interactions help disrupt the intermolecular forces holding lignin and xylan together, promoting their solubilization and removal during the pretreatment process.<sup>59,118</sup> In contrast, RDG offers a quantitative analysis, depicting gradients of H-bonding (blue) and H-repulsive sites (red) based on solvent energy distribution.<sup>117</sup> Throughout this investigation, van der Waals energy (white) acts as an intermediary state between H-bonding and H-repulsive interactions.<sup>117</sup>

In the context of solvent systems' interaction with VG (Fig. 12A), considerable variations in solvent energies were

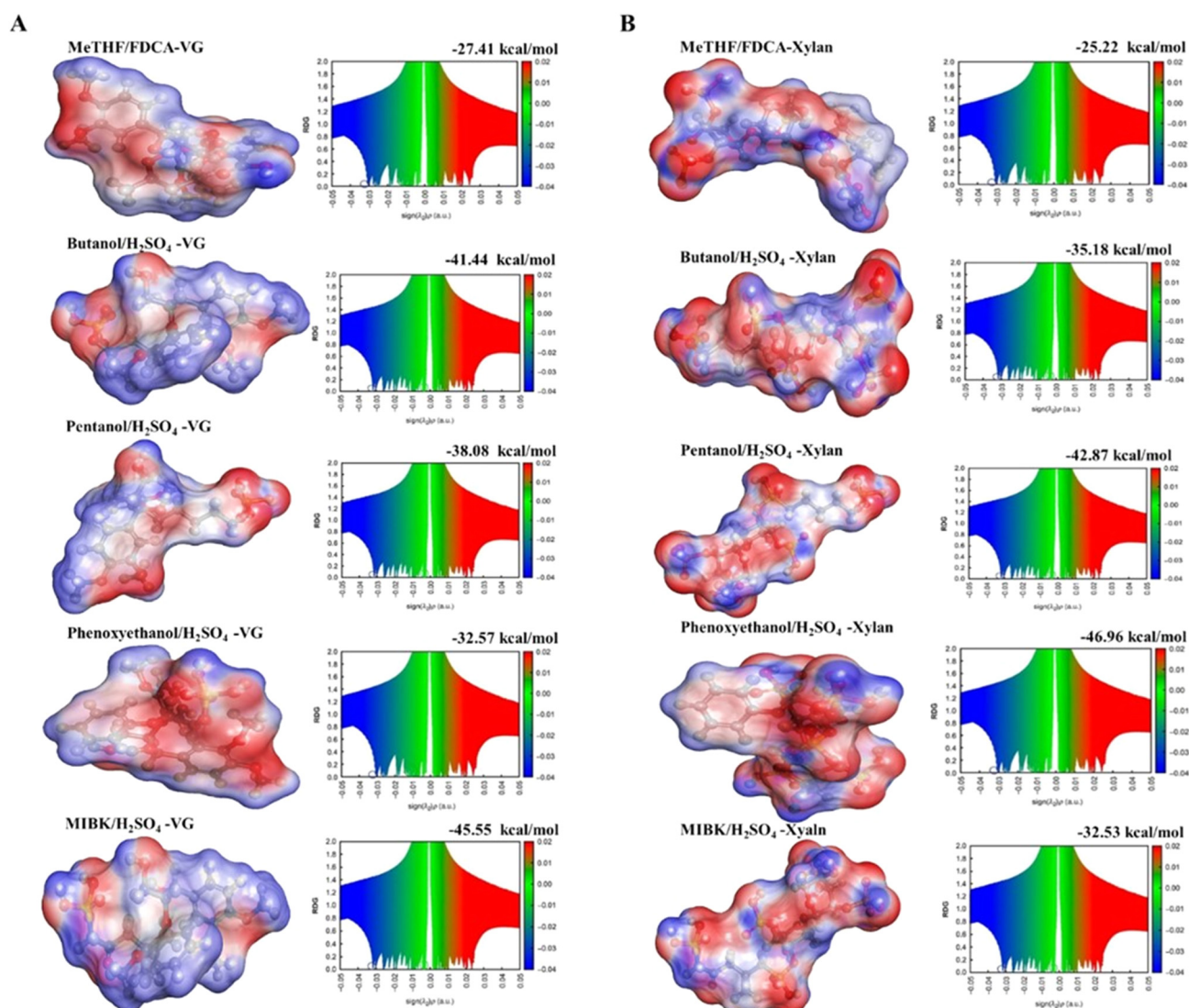


Fig. 12 Energy interaction potential of different biphasic solvent systems with VG (A) and D-xylan (B).

observed across the examined systems. The MIBK/H<sub>2</sub>SO<sub>4</sub>-VG system configuration notably exhibited the highest stability energy recorded at  $-45.55 \text{ kcal mol}^{-1}$ . This system displayed  $\text{sign}(\lambda_2)\rho$  values ranging from 0.017 to 0.05, alongside a robust RDG distribution spanning from 0.78 to 1.34 eV. These findings underscore its promising potential for applications in LCB fractionation. The 1-butanol/H<sub>2</sub>SO<sub>4</sub>-VG system competed closely, which demonstrated an energy level of  $-41.44 \text{ kcal mol}^{-1}$ .  $\text{sign}(\lambda_2)\rho$  values within this system fell between 0.023 and 0.05, accompanied by an RDG distribution ranging from 0.8 to 1.3 eV. Additionally, pentanol and phenoxyethanol emerged as noteworthy systems, with energy levels of  $-38.08$  and  $-32.57 \text{ kcal mol}^{-1}$ , respectively, when combined with VG and H<sub>2</sub>SO<sub>4</sub>. These systems, particularly those involving H<sub>2</sub>SO<sub>4</sub>, promote strong H-bonding interactions with VG, which play a significant role in the lignin separation process. The enhanced H-bonding helps weaken the lignin's internal cohesion and supports its dissolution into the solvent phase, thus improving the efficiency of lignin removal.<sup>43,59,118</sup> These comparative insights provide a critical perspective on solvent selection for optimizing the LCB fractionation process.

In terms of the interaction of solvent systems with D-xylan (Fig. 12B), the phenoxyethanol/H<sub>2</sub>SO<sub>4</sub> system exhibited the highest interaction energy of  $-46.96 \text{ kcal mol}^{-1}$ . Following this, the pentanol/H<sub>2</sub>SO<sub>4</sub> system showed interaction energies ranging between 0.023 and 0.05  $\text{sign}(\lambda_2)\rho$  and 0.025 and 0.05 eV for their corresponding RDG bands of 0.76 and 1.35, and 0.8 and 1.3 eV, respectively. Interestingly, 1-butanol and MIBK systems demonstrated lower  $\text{sign}(\lambda_2)\rho$  and RDG band values compared with pentanol. Specifically, in the cases involving VG and D-xylan, the MeTHF/FDCA solvent system exhibited the lowest interaction energies, measured at  $-27.41 \text{ kcal mol}^{-1}$  and  $-25.22 \text{ kcal mol}^{-1}$ , respectively (Fig. 12A and B). These results highlight how different solvent systems form distinct H-bonding networks with lignin and xylan, which could either facilitate or hinder their removal during fractionation.

Scientifically, these results highlight the varying affinities of different solvent systems towards VG and D-xylan, as evidenced by their interaction energies and related electronic parameters. The role played by H-bonding in these interactions is crucial, as it directly influences the separation and solubilization of lignin and xylan, both of which are essential for efficient biomass fractionation.<sup>59</sup> These findings suggest that the choice of solvent and its ability to form H-bonds with lignin and xylan can significantly affect the overall fractionation process. These are crucial for optimizing conditions in both lignin and xylan-related applications, including their extraction and valorization. Critically, while the study provides valuable data on the energetic landscapes of lignin and xylan-solvent interactions, further research could delve deeper into the structural dynamics and specific molecular interactions underlying these observed energy values.

## 4. Properties of different phases of biphasic fractionation

The present section provides a comprehensive elucidation of the three phases yielded by the biphasic pretreatment. It offers an in-depth exploration of the cellulose structure, the consequential effects of pretreatments on enzymatic hydrolysis efficiency, and the influence of transferred hemicelluloses and other compounds to the aqueous phase during fractionation. Furthermore, it examines the lignin fractionated from the organic phase and evaluates the impact of various pretreatment methodologies, solvent types, and operational conditions on lignin properties.

### 4.1. Undissolved solid phase

Cellulose, the most abundant polysaccharide in the undissolved solid phase after LCB pretreatment, plays a critical role in biorefinery production.<sup>119</sup> However, its crystalline structure, quantified by the crystallinity Index (CrI), significantly hinders enzymatic accessibility, ultimately limiting the efficiency of sugar conversion.<sup>120,121</sup> Understanding how pretreatment impacts cellulose crystallinity is essential for optimizing downstream processes in biorefineries.<sup>120</sup> In biphasic pretreatments, cellulose is typically recovered in the solid phase, facilitating its conversion into valuable platform sugars such as glucose *via* enzymatic hydrolysis.<sup>70</sup>

Madadi *et al.* employed CrI to assess how various solvent pretreatments (pentanol, ethanol, dioxane, 1-butanol) impact the crystalline structure of aspen cellulose. While all pretreatments increased CrI compared with raw biomass (57.0%), a CrI/cellulose ratio analysis indicated a slight decrease, suggesting the solvent-induced transformation of crystalline cellulose.<sup>121,122</sup> Notably, pentanol/H<sub>2</sub>SO<sub>4</sub> pretreatment resulted in the highest cellulose digestibility, potentially due to alterations in cellulose II crystallinity (parallel stacking disorder, lattice expansion, smoother surfaces). These findings suggest that pentanol and 1-butanol pretreatments promote enzyme accessibility and potentially glucose yield by removing polysaccharides and lignin, thereby loosening fibers and creating reactive sites on the biomass surface.<sup>43</sup> The cellulose surface analysis applied by scanning electron microscope shows 1-butanol effectively prevents lignin deposition on the surface unlike dilute acid pretreatment and exposes a more open and fibrous structure, potentially improving enzyme accessibility to cellulose. These findings warrant further investigation of the biphasic pretreatment for enhanced biofuel production from non-woody biomass.<sup>123</sup> In the other study during the pretreatment of eucalyptus with MIBK, the CrI was increased with the reaction temperature and produced cellulose-rich residues.<sup>124</sup> Also, it is essential to understand the impact of pretreatment on its structure and digestibility. Effective pretreatment methods that promote cellulose accessibility and efficient lignin removal are key for maximizing sugar yields in biorefineries.

Evaluating cellulose digestibility is a critical indicator of its potential valorization, with most recovered cellulose pulps

exhibiting favorable digestibility rates of approximately 80.0% or higher.<sup>42</sup> This high digestibility is primarily attributed to removing lignin and hemicellulose, which improves cellulase accessibility to cellulose.<sup>119</sup> Effective delignification is crucial as its complex aromatic structure intertwines with cellulose fibers, hindering enzyme access and promoting non-productive enzyme binding.<sup>125</sup> Consequently, inefficient delignification during pretreatment significantly reduces enzymatic hydrolysis efficiency, underscoring its importance for enhanced cellulose digestibility.<sup>43,70</sup> Studies have shown that adding certain ions like  $\text{Cl}^-$  and  $\text{Br}^-$  can accelerate the hydrolysis rates of glycosidic bonds.  $\text{Br}^-$  anions might catalyze the cleavage of these bonds by facilitating nucleophilic attacks.<sup>126</sup> However, an excess of chloride ions can also hasten condensation reactions, resulting in the formation of humins that can deposit onto cellulose, thereby reducing its digestibility.<sup>127</sup> It is important to note that utilizing  $\text{FeCl}_3$  and  $\text{HCl}$  in the MeTHF system caused severe cellulose degradation, highlighting the complexity of solvent systems in biomass conversion.<sup>82</sup> In contrast, the  $\text{AlCl}_3$ -catalyzed system with  $\text{NaCl}$  demonstrated a lesser influence on residue composition and reduced cellulose degradation.<sup>86</sup> Conversely, the literature mentions mannitol as a potential additive to deter lignin accumulation on cellulose surfaces and improve cellulose digestibility.<sup>44</sup>

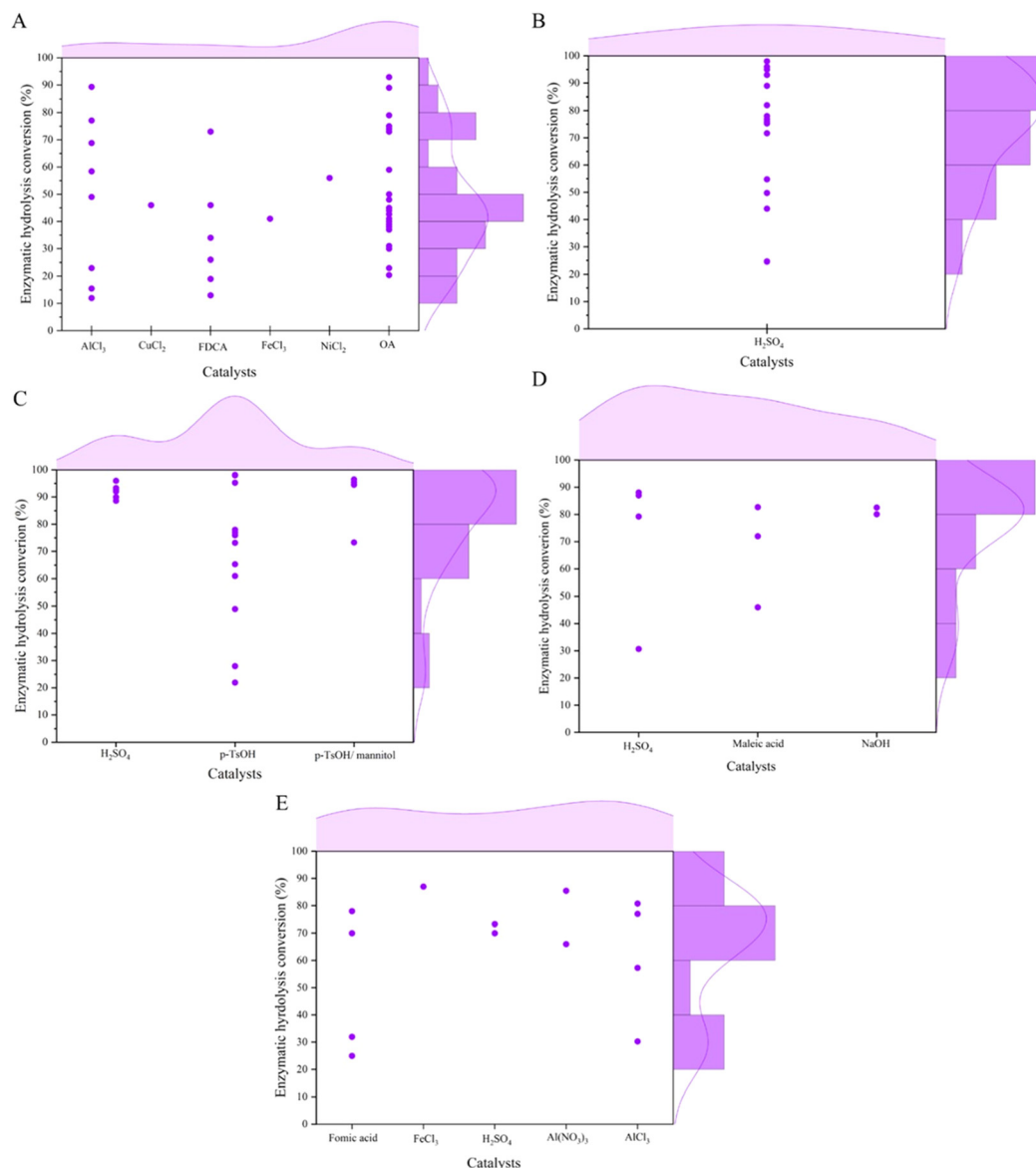
**4.1.1. Enzymatic hydrolysis.** The effectiveness of LCB fractionation is highly dependent on the chosen pretreatment method and its impact on the individual components. This section explores how various pretreatment catalysts influence the subsequent enzymatic hydrolysis conversion efficiency. By understanding these catalyst effects, researchers can optimize pretreatment strategies to maximize sugar yield and overall biorefinery efficiency.

Fig. 13 shows the scatter plot visualizing the enzymatic hydrolysis conversion (%) achieved with various solvent systems. Notably, the solid fraction from each biphasic pretreatment exhibited an average digestibility, regardless of the enzyme type or activity used. The solid fraction from the MeTHF system exhibited an average digestibility of 50.0% (Fig. 13A). The plot shows that OA is more frequently used than other catalysts, with reported hydrolysis rates exceeding 90.0%; after that,  $\text{AlCl}_3$  follows closely behind in terms of effectiveness. The shaded area behind the data points depicts the range of variability in hydrolysis rates observed for each catalyst, along with the average rate. The solid fraction obtained from the 1-butanol system using  $\text{H}_2\text{SO}_4$  exhibited a higher average digestibility (~85.0%) and a tendency toward increased conversion rates (ranging from 90.0% to 100%) (Fig. 13B). While the pentanol system employing  $\text{H}_2\text{SO}_4$ , *p*-TsOH, and *p*-TSOH-mannitol achieved a higher average digestibility of 80.0%, *p*-TsOH, the most frequently used catalyst in this study, exhibited a multimodal distribution in terms of digestibility (Fig. 13C). Conversely,  $\text{H}_2\text{SO}_4$  displayed a tendency towards achieving higher conversion rates (ranging from 90.0 to 100%). Fig. 13D depicts the solid conversion of the phenoxyethanol system. Although the number of studies is limited, this system achieved an average digestibility of 85.0%. Interestingly,  $\text{H}_2\text{SO}_4$

appears to be the most frequently investigated catalyst, and it also demonstrates a tendency towards higher conversion rates, exceeding 80.0% in most cases. Fig. 13E presents the average digestibility (ranging from 60.0% to 80.0%) achieved by the MIBK system with various catalysts, including  $\text{FeCl}_3$ ,  $\text{AlCl}_3$ ,  $\text{H}_2\text{SO}_4$ ,  $\text{Al}(\text{NO}_3)_3$ , and formic acid. While  $\text{AlCl}_3$  and formic acid appear to be the most frequently studied catalysts in this system,  $\text{H}_2\text{SO}_4$  stands out by achieving a considerably higher conversion rate, approaching 90.0%.

Solid loading is also a critical factor influencing the efficiency of converting cellulose to glucose during enzymatic hydrolysis.<sup>128</sup> This concept is explored in Fig. 14, which examines the effect of varying solid loadings (Table S2†). Cellulose conversion relies heavily on enzyme activity and the combined action of enzymes like endoglucanase (EG),  $\beta$ -glucosidase (BG),  $\alpha$ -amylase,  $\beta$ -amylase, and xylanase. These enzymes work together synergistically in enzyme cocktails to efficiently convert cellulose into glucose.<sup>128</sup> However, using high solid loading presents challenges. Increased viscosity, mass transfer limitations, and inadequate mixing can all hinder hydrolysis efficiency.<sup>128–130</sup> Conversely, lower solid loadings lead to lower viscosity, allowing for better mixing and mass transfer. This can potentially increase hydrolysis rates.<sup>130,131</sup> The NREL protocol, a widely used standard in enzymatic hydrolysis, recommends 48 to 72 h of hydrolysis at temperatures ranging from 45 to 50 °C, depending on the specific enzyme cocktail used.<sup>132</sup> Fig. 14 utilizes a violin plot to graphically represent enzymatic hydrolysis rates across various solid loadings (Fig. 14A–E). Each violin shape depicts the distribution of hydrolysis rates at different loadings. The wider the violin, the higher the frequency or probability density of data points at that concentration. The y-axis shows the enzymatic hydrolysis rate relative to the solid loading, ranging from 0.0% to 100%, enabling easy comparison across different conditions. The violin plots within the graph not only elucidate the central tendency and variability of the data but also provide a visual estimation of the density of data points, thereby offering a comprehensive overview of the distribution across different solid loadings.

Fig. 14A displays enzymatic hydrolysis of the MeTHF-pretreated system conducted at four different solid loadings (2.0%, 2.5%, 6.0%, and 8.0%). These color-coded and sized violins visually summarize the data distribution at their respective concentrations. A key feature of the violin plot is the white dot within each violin, representing the median hydrolysis rate for each solid loading percentage. The median, less affected by outliers than the mean, is a reliable measure of central tendency. By analyzing differences in violin width, median, and interquartile range (IQR), we gain insights into how solid loading influences enzymatic hydrolysis rate. The plot reveals that the highest median rate occurs at the 2.5% solid loading, suggesting this concentration might be optimal for enzymatic hydrolysis. At this concentration, the median hydrolysis rate is around 65.0%. Additionally, the black bars represent the interquartile ranges, which offer insights into data variability. Wider ranges indicate greater dispersion of



**Fig. 13** Scatter plot illustrating the enzymatic hydrolysis (%) across different catalysts. The X-axis represents the catalyst type, and the Y-axis shows the cellulose conversion rate. Each dot in the scatter plot represents the conversion rate obtained with a specific catalyst. The shaded area along the X-axis depicts the distribution of the conversion rates across all catalysts. Similarly, the shaded area on the Y-axis represents the distribution of the different catalyst types used in the experiment. (A) MeTHF, (B) butanol, (C) pentanol, (D) phenoxyethanol, and (E) MIBK. The data in the scatter plot are based on the literature review summarized in Table S2.†

hydrolysis rates. The violin at 2.0% solid loading exemplifies this, with an IQR suggesting a spread of almost 40.0% in hydrolysis rate. The plot suggests that increasing solid loading initially correlates with higher enzymatic hydrolysis rates. However, beyond a certain point (optimal point), the rate does not increase proportionally, as observed at the 8.0% solid loading. This highlights the importance of finding the right balance between solid loading and hydrolysis efficiency.

Fig. 14B displays enzymatic hydrolysis of the 1-butanol-pre-treated system at 2.0%, 9.0%, 10.0%, and 13.0% solid loadings. The median conversion efficiency at 2.0% solid loading is visually deduced to be approximately 50.0%, with an IQR

spanning from 40.0% to 60.0%. Progressing to 9.0% solid loading, the median conversion is observed at nearly 70.0%, and the IQR extends from 60.0% to 80.0%. At a solid loading of 10.0%, the median conversion rate increases to roughly 80.0%, with an IQR between 70.0% and 90.0%. The highest solid loading evaluated, 13.0%, exhibits a median conversion rate close to 90.0%, with an IQR from 80.0% to 100%. The violin plots within the graph not only elucidate the central tendency and variability of the data but also provide a visual estimation of the density of data points, thereby offering a comprehensive overview of the distribution across different solid loadings.

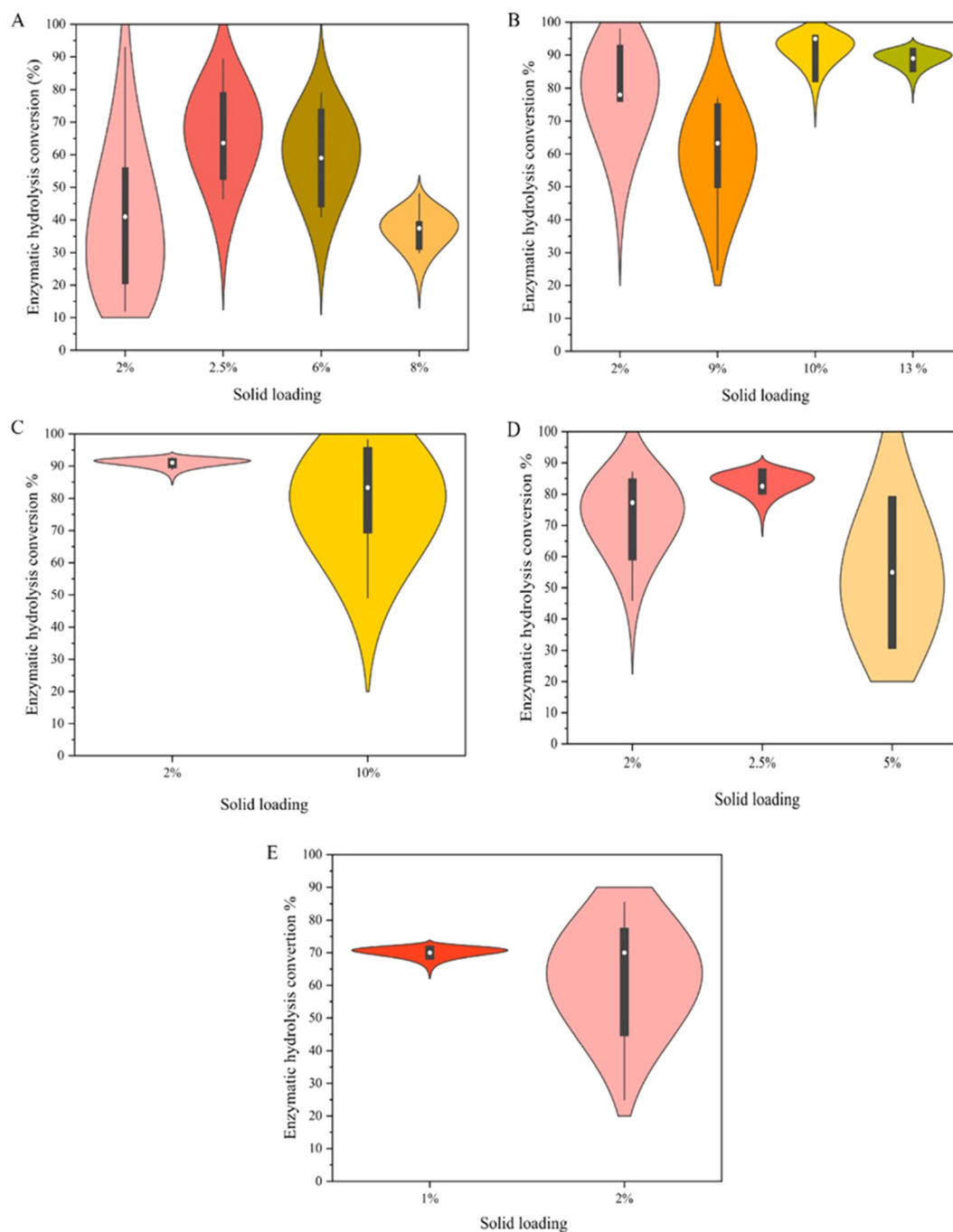


**Fig. 14** Violin plot showing the distribution of solid loading in biphasic solvent systems. (A) MeTHF, (B) butanol, (C) pentanol, (D) phenoxyethanol, and (E) MIBK. The data are based on the literature review summarized in Table S2.†

Fig. 14C delineates two violin plots representing the enzymatic hydrolysis conversion at solid loadings of 2.0% and 10.0% in the pentanol-pretreated system. The 2.0% solid loading plot exhibits a narrow configuration with a pronounced peak, suggesting a high density of data points clustered around a superior conversion percentage. This infers a consistent enzymatic hydrolysis performance at this loading level. The median value is indicated by a white dot, positioned

near the apex of the plot, signifying a central tendency towards higher conversion percentages. Conversely, the 10.0% solid loading plot manifests a broader shape with a lower tail, denoting a wider distribution of conversion percentages and a bimodal data point clustering—one at a higher conversion rate and another at a lower rate. This indicates a variability in the enzymatic hydrolysis outcomes at this concentration. The median value is observed at a lower position (85.0%) compared

with the 2.0% plot, reflecting the diverse range of conversion efficiencies.

Fig. 14D displays four violins corresponding to 2.0%, 2.5%, and 5.0% solid loadings in the phenoxyethanol-pretreated system. The 2.0% solid loading exhibits a broader IQR, suggesting greater variability in enzymatic efficiency, whereas the 2.5% solid loading shows a narrower and taller distribution, indicating a more consistent performance. The 5.0% solid loading, with its wider distribution, implies increased variance, which could be attributed to factors such as substrate inhibition or diffusional limitations at higher solid concentrations. The median value is observed at 55.0% for 5.0%, 78.0% for 2.0%, and 82.0% for 2.5%.

In Fig. 14E, the violin plot compares the enzymatic hydrolysis for two different solid loadings, 1.0%, and 2.0%, in the MIBK-pretreated systems. The median conversion percentage for 1.0% solid loading is approximately 55.0%, indicated by a white dot, and it has a narrower IQR, suggesting a more consistent data set with less variability. In contrast, the 2.0% solid loading shows a median conversion percentage closer to 80.0%, with a broader IQR, indicating a higher variability among the data points. The density of the data is represented by the width of the violins; the 1.0% solid loading has a slimmer profile, reflecting fewer data points at varying conversion percentages, while the 2.0% solid loading has a wider profile, suggesting a greater number of data points spread across the conversion percentages. This visual representation implies that increasing the solid loading from 1.0% to 2.0% not only increases the median enzymatic hydrolysis conversion percentage but also introduces more variability into the process. The plot effectively illustrates the trade-off between efficiency and consistency in the enzymatic hydrolysis process at different solid loadings.

The analysis of enzymatic hydrolysis modeling underscores the significant impact of pretreatment catalysts and solid loadings on conversion efficiency. Systems employing  $\text{H}_2\text{SO}_4$  as a catalyst consistently demonstrated high digestibility across various solvents, notably in 1-butanol and phenoxyethanol systems, suggesting its effectiveness in enhancing enzymatic hydrolysis rates. Additionally, the study reveals that intermediate solid loadings offer an optimal balance, improving hydrolysis efficiency by enhancing mixing and mass transfer while avoiding the challenges associated with high solid loadings. Therefore, future research and industrial applications should prioritize the use of  $\text{H}_2\text{SO}_4$  as a catalyst, particularly in 1-butanol and pentanol systems, combined with intermediate solid loadings to achieve superior and consistent enzymatic hydrolysis performance.

#### 4.2. Dissolved component in the aqueous phase

Hemicellulose, a complex biopolymer composed of uronic acids, pentose sugars (arabinose and xylose), acetyl groups, and various saccharide units, can be depolymerized using biphasic systems to yield valuable products.<sup>133,134</sup> Biphasic systems promote the breakdown of hemicellulose chains, liberating fermentable monosaccharides (pentoses and hexoses) and poten-

tially xylooligosaccharides (XOS) depending on the reaction conditions.<sup>104</sup> Therefore, the ability of solvents under operational pretreatment conditions (time and temperature) and the effect of catalysts alongside them on the amount of hemicellulose removal in biphasic pretreatment is considered crucial.

Extracting valuable C5 sugars from LCB, a key biofuel building block, requires a delicate balance. While harsher conditions (higher temperature, longer time, stronger catalysts) boost C5 sugar yields, they also degrade hemicellulose to FF.<sup>79,134</sup> Fig. 14 depicts the key steps involved in the formation of FF from hemicellulose. Biphasic systems like MeTHF/OA (bamboo-derived) achieve high hemicellulose removal at moderate temperatures but also generate furans.<sup>135,136</sup> Conversely, milder conditions with weak organic acids favor higher hemicellulose recovery and potentially XOS production or leave unhydrolyzed hemicellulose.<sup>65</sup> An FDCA catalyst system offers high hemicellulose removal at milder temperatures but suffers from extended reaction times that promote FF formation.<sup>78,88</sup> Toluene/ $\text{H}_2\text{SO}_4$  systems were identified as well suited for efficient FF production. This system achieved impressive FF yields (65.6%) in just 10 minutes, even with high solid loading. The application of pressure significantly enhanced the process. Additionally, the high FF content in the toluene phase after the reaction simplified FF separation and purification.<sup>137</sup> Conversely,  $\text{AlCl}_3$  offered a balance between FF yield and cellulose preservation.<sup>92</sup> Additionally, NaCl was found to significantly enhance FF yield from xylose in Brønsted acid-catalyzed reactions.<sup>92</sup> Li *et al.* established a method for concurrently generating FF (56.6%) and cellulose (90.0%) from sugarcane bagasse, scrutinizing the degradation processes within a single aqueous and MeTHF/ $\text{AlCl}_3$  system.<sup>86</sup> Within the MIBK system, the conversion yields of 37.0% HMF and 35.0% FF from bamboo culm and 35.0% HMF and 34.0% FF from bamboo leaves were obtained and inhibited the formation of unwanted solid particles by unwanted polymerization reactions.<sup>138</sup> This contrasts with the promising effect of  $\text{AlCl}_3$ , which maintained a significant FF yield (70.3%) and mitigated cellulose degradation, hinting at its potential in future LCB fractionation.<sup>109</sup>

Organic solvents in biphasic systems notably influence the thermodynamics of reactants, catalysts, and products involved in furan compound production, leading to higher FF yields compared with aqueous systems.<sup>52</sup> FF and its isomer HMF are prone to degradation and require careful separation from the biphasic systems. Also, organic solvent properties significantly influence FF formation and separation. Lower solvation free energy in the organic phase favors FF selectivity, while FF degradation in the aqueous phase and the partition coefficient also play a role.<sup>139</sup> Ultimately, the pretreatment conditions are tailored to the desired product outcome, whether it be maximizing sugar recovery or furan generation. Moreover, Brønsted acid sites drive LCB hydrolysis to fermentable sugars and fructose dehydration to HMF, highlighting the importance of catalyst Brønsted acidity for these biomass conversion reactions.<sup>95</sup>

In their quest to convert cellulose into the valuable biofuel precursor HMF, researchers explored using metal chlorides as

catalysts. While some catalysts favored unwanted byproducts, others showed promise.  $\text{MoCl}_3$  and  $\text{CrCl}_3$ , though generating HMF, also produced lactic acid through an undesired pathway. The researchers then focused on  $\text{FeCl}_3$ ,  $\text{RuCl}_3$ ,  $\text{TiCl}_3$ , and  $\text{VCl}_3$ , testing them in a two-phase system with a salt solution and an organic solvent. This aimed to boost HMF yield by extracting it from the water layer. Among the tested solvents, 1-butanol emerged as the champion, maximizing HMF selectivity (75.2–87.5%) likely due to its ability to suppress unwanted reactions in the water phase.<sup>140</sup> Further exploration within this optimized system revealed  $\text{RuCl}_3$  to be the star performer, achieving an impressive yield (87.5%) and selectivity (83.3%) for HMF.<sup>140</sup> This study highlights the synergistic effect of  $\text{RuCl}_3$  and the chosen biphasic system in significantly reducing HMF degradation, paving the way for a promising one-pot method for HMF production.<sup>140</sup> In addition, a two-phase system using  $\text{FeCl}_3$ – $\text{CuCl}_2$  catalyst effectively converted cellulose into HMF (49.1 wt%) and furan derivatives (2.9 wt%) at 190 °C for 45 minutes. This approach avoids rehydration of HMF through extraction into the organic phase and exhibits lower activation energy (21.6 kJ mol<sup>-1</sup>) compared with inorganic acid catalysts, enabling a faster reaction rate at moderate temperatures. The metal chlorides break hydrogen bonds in cellulose, and  $\text{CuCl}_2$  promotes the dehydration of HMF and derivatives.<sup>110</sup>

#### 4.3. Structure and components of the organic phase

Lignin, a complex plant polymer, has diverse inter-unit linkages (ether & C–C bonds) that vary by plant source.<sup>141</sup> Fig. 15 presents the chemical macromolecular structure of lignin and inter-unit linkage. Also, Table 3 provides a detailed overview of the linkage distribution across various LCB feedstocks. As illustrated in Fig. 15 and Table 3, the  $\beta$ -O-4 ether linkage is the predominant bond type within lignin. Acidic environments, used in LCB processing, break down lignin but can also trigger re-polymerization into denser, problematic structures during saccharification, hindering further processing.<sup>35,142</sup> Biphasic systems disrupt the LCC,<sup>143</sup> facilitating the solubilization of larger lignin fragments into oligomers.<sup>141</sup> Further degradation of these oligomers occurs through cleavage of  $\beta$ -O-4 linkages, often aided by acid or base catalysts.<sup>144</sup> However, this process

**Table 3** Distribution of lignin linkages in various LCB feedstock<sup>141</sup>

Linkage	LCB types (%)		
	Softwood	Hardwood	Grasses
$\beta$ -Aryl ether ( $\beta$ -O-4)	45.0–50.0	60.0–62.0	74.0–84.0
Phenylcoumaran ( $\beta$ -5) and ( $\alpha$ -O-4)	9.0–12.0	3.0–11.0	5.0–11.0
Resinol ( $\beta$ - $\beta$ ) and ( $\alpha$ -O- $\gamma$ )	2.0–6.0	3.0–12.0	1.0–7.0
Diaryl ether (4-O-5)	4.0	4.0–7.0	N/A
Biphenyl (5-5)	10.0–25.0	4.0–10.0	N/A
1,2-Diarylpropane ( $\beta$ -1)	3.0–7.0	5.0–7.0	N/A

can be a double-edged sword. While acid promotes cleavage, it can also trigger undesirable re-polymerization into denser structures during saccharification, hindering further processing.<sup>141</sup> The extent of both cleavage and re-polymerization increases with harsher pretreatment conditions (Fig. 16).<sup>141</sup>

Physicochemical characterization of isolated lignin is essential for assessing pretreatment efficacy, elucidating lignin structure, and designing valuable applications. Lignin molecular weight ( $M_w$ ) and number-average molecular weight ( $M_n$ ) directly correlate with  $\beta$ -aryl ether content, revealing that biphasic systems effectively stabilize lignin during decomposition, yielding a highly reactive product.<sup>59,141</sup> However, the observed increase in polydispersity index (PDI,  $M_w/M_n$ ) indicates a reduction in lignin uniformity after pretreatment. Additionally, pretreatment effectively disrupts LCCs, resulting in exceptionally high lignin purity, as quantified by sugar analysis, and concomitantly enhancing carbohydrate accessibility (Table 4).

The ideal outcome is a low-molecular-weight lignin with high solubility in various organic solvents.<sup>42</sup> This allows for efficient downstream conversion into valuable products like 2-methoxyphenol and 2,6-dimethoxyphenol.<sup>152</sup> Notably, organic solvents can remove over 60.0% of lignin compared with just 20.0% in the aqueous phase, highlighting their effectiveness.<sup>139,141</sup> The choice of solvent and extraction conditions significantly impacts the characteristics of the isolated lignin. Increasing extraction temperature generally decreases lignin molecular weight and  $\beta$ -O-4 content due to acidic cleavage, but this can also lead to the loss of some acid-sensitive structures.<sup>153,154</sup> Chlorinated hydrocarbons, for example, have

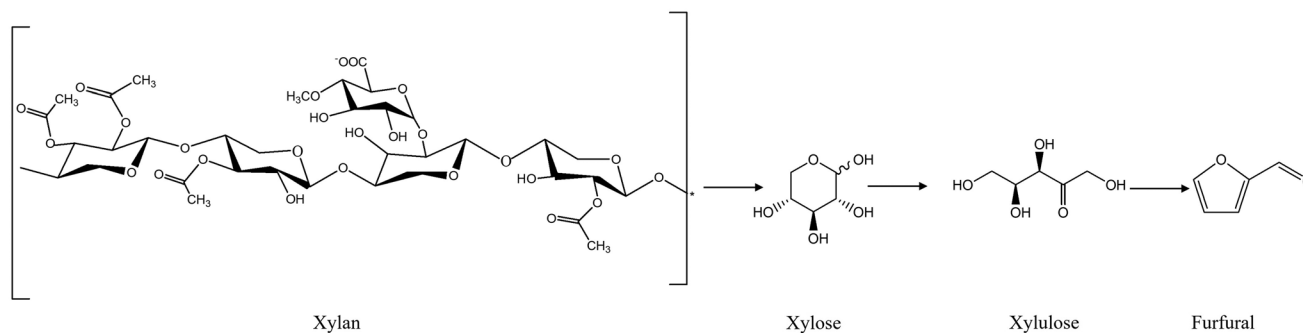


**Fig. 15** Proposed pathway for hemicellulose conversion to FF. Reproduced from reference Lu et al.<sup>145</sup> with permission from Elsevier. Copyright©2025. (LN: 5976551179971).

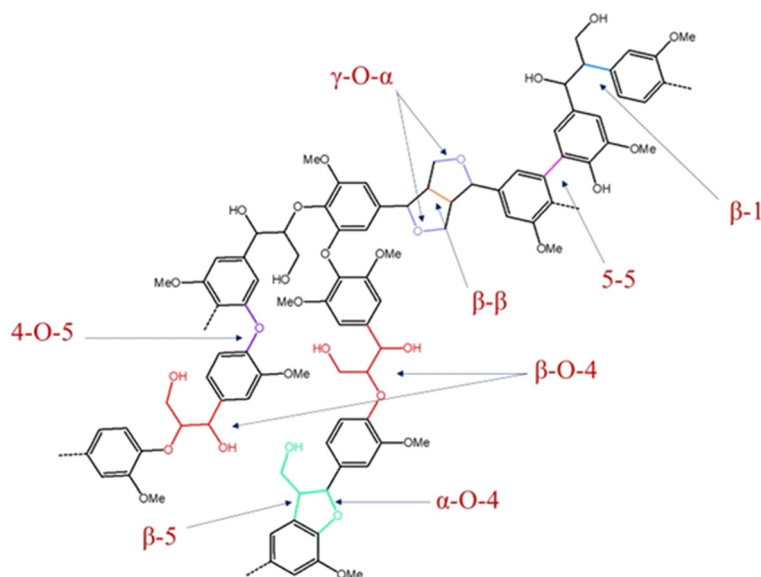


Fig. 16 Schematic representation of lignin's macromolecular structure highlighting key inter-unit linkages.<sup>141</sup>

Table 4 Expected lignin properties from the organic phase of biphasic solvent systems. N/A, not available

Pretreatment	$\beta$ -O-4 (per 100 Ar)	Purity (%)	Molecular weight ( $\text{g mol}^{-1}$ )			Ref.
			$M_w$	$M_n$	$M_w/M_n$	
MeTHF/ $\text{AlCl}_3$	40.4	99.5	1278	744	1.7	59
MeTHF/ $\text{AlCl}_3$	N/A	99.6	2289	860	2.6	82
MeTHF/ $\text{AlCl}_3$	N/A	99.5	1656	787	2.1	82
MeTHF/ $\text{AlCl}_3$	N/A	98.8	4172	1046	4.0	82
MeTHF/FDCA	45.0	N/A	1600	N/A	N/A	78
MeTHF/FDCA	23.0	N/A	1900	N/A	N/A	78
MeTHF/HCl	16.0	N/A	2100	1200	1.7	85
MeTHF/OA	43.0	N/A	1600	N/A	N/A	78
MeTHF/OA	52.0	N/A	1400	N/A	N/A	78
MeTHF/OA	36.0	N/A	2600	N/A	N/A	78
MeTHF/OA	73.0	97.6	3730	1840	2.0	87
MeTHF/OA	63.0	99.3	2240	1430	1.6	87
MeTHF/OA	61.0	99.2	2690	1510	1.8	87
MeTHF/ <i>p</i> -TsOH	47.0	N/A	1995	833	2.4	79
MeTHF/ <i>p</i> -TsOH	22.0	N/A	1900	814	2.3	79
MeTHF/ <i>p</i> -TsOH	9.30	N/A	1676	717	2.3	79
1-Butanol/ $\text{H}_2\text{SO}_4$	12.3	99.3	1304	754	1.7	59
1-Butanol/ $\text{H}_2\text{SO}_4$	27.3	97.2	6360	1381	4.6	43
1-Butanol/ $\text{H}_2\text{SO}_4$	N/A	94.0	11 270	1457	7.7	146
1-Butanol/ $\text{H}_2\text{SO}_4$	N/A	85.0	3180	699	4.5	63
Pentanol/ $\text{H}_2\text{SO}_4$	64.0	98.1	7621	1515	5.0	43
Pentanol/ $\text{H}_2\text{SO}_4$	42.5	57.1	N/A	N/A	N/A	41
Pentanol/ <i>p</i> -TsOH	42.4	99.5	1254	813	1.5	59
Pentanol/ <i>p</i> -TsOH	61.5	99.0	4241	2401	1.7	44
Pentano/ <i>p</i> -TsOH	47.3	99.0	2815	1704	1.6	46
Phenoxyethanol/ $\text{H}_2\text{SO}_4$	N/A	89.0	4632	3686	1.2	105
Phenoxyethanol/ $\text{H}_2\text{SO}_4$	N/A	91.3	4809	3000	1.6	105
Phenoxyethanol/ $\text{H}_2\text{SO}_4$	N/A	84.8	4247	3306	1.3	105
Phenoxyethanol/ $\text{H}_2\text{SO}_4$	11.0	N/A	N/A	N/A	N/A	147
Phenoxyethanol/ $\text{H}_2\text{SO}_4$	5.2	N/A	N/A	N/A	N/A	147
Phenoxyethanol/ $\text{H}_2\text{SO}_4$	N/A	92.2	435	421	1.0	148
Phenoxyethanol/ $\text{H}_2\text{SO}_4$	N/A	90.2	504	488	1.0	148
Phenoxyethanol/ $\text{H}_2\text{SO}_4$	N/A	90.0	562	531	1.0	148
Phenoxyethanol/ $\text{H}_2\text{SO}_4$	12.7	91.9	4975	3525	1.4	149
MIBK/FDCA	24.0	N/A	N/A	N/A	N/A	88
MIBK/ $\text{FeCl}_3$	40.3	100	1227	767	1.6	150
MIBK/ $\text{H}_2\text{SO}_4$	N/A	N/A	10 800	4500	2.4	151

been shown to protect  $\beta$ -O-4 bonds better than 1-butanol during acidic extraction.<sup>153</sup> However, 1-butanol suffers from another drawback: its presence in water promotes  $\beta$ -O-4 cleavage, reducing its effectiveness in the 1-butanol/H<sub>2</sub>SO<sub>4</sub> process.<sup>98</sup> Interestingly, a higher 1-butanol-to-water ratio might improve  $\beta$ -O-4 preservation, suggesting further optimization possibilities.<sup>59</sup>

Aliphatic alcohol solvents like 1-butanol can introduce another complication – lignin etherification.<sup>22</sup> This reaction involves the formation of etherified lignin structures and is reversible under mildly acidic conditions.<sup>39,40</sup> While 1-butanol/H<sub>2</sub>SO<sub>4</sub> achieves a good lignin removal rate (70.0%) along with high hemicellulose removal (85.0%), it suffers from promoting  $\beta$ -O-4 cleavage, reducing its effectiveness in preserving these key structural components.<sup>101,155,156</sup> Pentanol offers a superior alternative, protecting  $\beta$ -O-4 linkages likely due to its ability to prevent C–C bond formation.<sup>43</sup>

Pretreatment success can also be evaluated by analyzing the  $\beta$ -O-4 content, a crucial structural feature.<sup>43,157</sup> Techniques like pentanol/*p*-TsOH and MeTHF/AlCl<sub>3</sub> have demonstrated efficient  $\beta$ -O-4 preservation (40.0–42.0%) with minimal sugar contamination and consistent molecular weight.<sup>39,59</sup> These systems also yielded high quantities of phenolic monomers following catalytic hydrogenolysis, suggesting efficient lignin depolymerization.<sup>59</sup> Analysis of the aromatic region further revealed the presence of specific lignin units and suggested

that the biphasic systems promoted condensation reactions at targeted positions.<sup>39</sup> Notably, the pentanol/*p*-TsOH system displayed a higher ratio of these units, potentially indicating more efficient lignin extraction. Finally, biphasic lignin exhibited lower aliphatic group content due to  $\beta$ -O-4 cleavage but displayed increased phenolic hydroxyl content, highlighting lignin depolymerization during separation. This enhanced presence of both functional groups underscores the potential of biphasic lignin for various applications.<sup>59</sup>

For instance, Xie *et al.* investigated the catalytic hydrogenolysis of various lignin samples to produce valuable aromatic compounds.<sup>59</sup> The resulting product distribution, as depicted in Fig. 17, primarily consisted of phenolic monomers, with 4-propyl syringol (Pr-S, 43.4 to 50.3%), 4-ethyl syringol (Et-S, 45.6–48.6%) as the dominant compounds. Smaller amounts of 4-propyl guaiacol (Pr-G, 0.5 to 4.0%) and 4-ethyl guaiacol (Et-G, 0.7–2.4%) were also identified. Product selectivity was influenced by reaction conditions, with phenolic compounds derived from syringyl (S) units generally predominating due to their higher abundance in hardwood lignin and lignin richer in  $\beta$ -O-4 linkages, which has been shown to yield a higher proportion of aromatic monomers.<sup>59</sup>

In conclusion, biphasic systems, combining water-immiscible solvents with high lignin solubility and acidic catalysts, offer a promising approach for lignin valorization. These systems effectively protect  $\beta$ -O-4 linkages, leading to the iso-

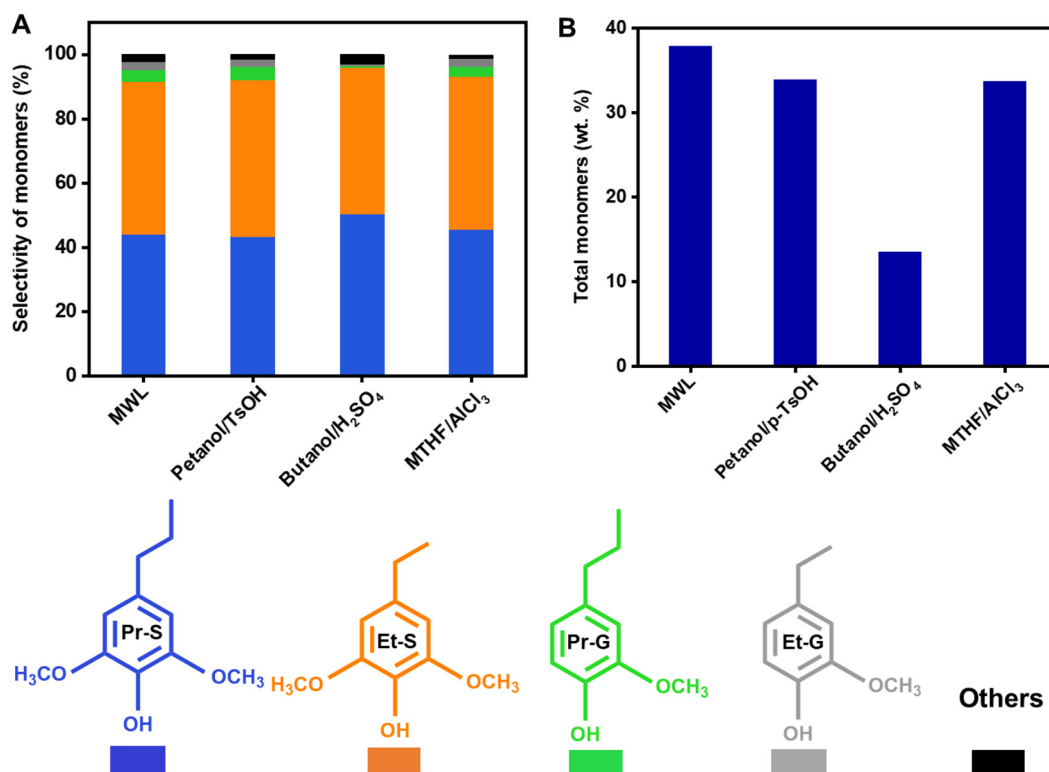


**Fig. 17** Phenolic monomer profile obtained from catalytic hydrogenolysis of pentanol/*p*-TsOH, MTHF/AlCl<sub>3</sub>, and butanol/H<sub>2</sub>SO<sub>4</sub> lignin samples. The primary products identified include 4-propyl syringol (Pr-S), 4-ethyl syringol (Et-S), 4-propyl guaiacol (Pr-G), and 4-ethyl guaiacol (Et-G). Phenolic monomer selectivity (A) and total monomer yield (A) were obtained from catalytic hydrogenolysis of WML and biphasic lignin samples.<sup>59</sup> With permission from Elsevier. Copyright©2024. (LN: 5847790555922).

lation of native-like lignin with high potential as a feedstock for aromatic monomer production. Further optimization is crucial to maximizing  $\beta$ -O-4 preservation, and factors such as biomass particle size, stirring speed, solvent ratios, and extraction temperature require investigation. The ability to selectively fractionate lignin based on molecular weight through biphasic systems offers additional advantages. By tailoring the solvent system to the desired final product, biphasic technology provides a versatile and efficient platform for lignin biorefineries.

## 5. Impact of recovered solvents – catalysts on lignocellulosic biomass fractionation

The high cost of solvents and catalysts can impair the economic viability of biphasic systems, hindering their widespread use in industry.<sup>42,57,118</sup> The biphasic solvent systems, after fractionation, naturally separate into two distinct phases, making layer separation easier than in other organosolv processes. This results in significantly lower energy requirements for solvent separation and recycling, reducing both cost and energy consumption compared with traditional monophasic systems.<sup>60,118</sup> Efficient recovery and reuse of these materials allow biphasic systems to overcome the cost barrier. Recent research has shown the feasibility of this approach, paving the way for more economical biphasic processes.<sup>123</sup> In simpler terms, recycling allows biphasic systems to capitalize on their inherent energy efficiency and unlock the full potential of high-performance catalysts and solvents, making them a much more attractive option for large-scale industrial applications.<sup>7</sup> Solvents can be recovered using rotary vacuum evaporation and catalyst recovery depends on the catalyst type (homogeneous or heterogeneous). Homogeneous catalysts may precipitate from the concentrated solution, while heterogeneous catalysts can often be filtered and recycled after solvent removal.<sup>40,43</sup>

### 5.1. Solvent recovery

Several studies have explored the feasibility of recycling solvents used in LCB pretreatment. Pentanol recycling demonstrates significant promise. An initial study reported a high recycling efficiency of 97.0%, dropping slightly to 84.0% by the fourth cycle.<sup>43</sup> While the recycled pentanol maintained effectiveness in cellulose digestibility (81.0% compared with the initial 94.0%) and delignification (71.0% compared with 80.0%), a decrease in efficiency with each cycle was observed. This is likely due to the accumulation of dissolved sugars and lignin in the recycled solvent, potentially modifying its structure. Recycling phenoxyethanol for three cycles achieved an impressive 80.6% delignification and a 71.2% enzymatic digestibility of the cellulose, showing no significant difference compared with using the fresh solvent.<sup>103</sup> Also, researchers investigated the reusability of MIBK in FF production. The MIBK was successfully recovered and achieved stable FF yields

of ~75.0% after 5 runs.<sup>158</sup> Cheng *et al.* reported successful 1-butanol recycling, achieving a yield exceeding 90% in each cycle.<sup>159</sup> Notably, even after the third cycle, a high recovered solid yield (49.0%) was obtained with excellent lignin removal (65.1%). Similarly, another study utilizing recycled 1-butanol achieved a remarkable 64.6% molar yield through acidic processing.<sup>63</sup>

Further research suggests that while solvent recycling can be efficient, some limitations exist. After three cycles, the residual solid yield remained constant in one study, but the hemicellulose separation rate decreased from 51.3% to 40.8%.<sup>160</sup> This decrease was attributed to the accumulation of impurities in the recycled solvents. Another study investigating phenoxyethanol for pretreating bamboo residues reported a slight decrease in cellulose-to-sugar conversion efficiency with each reuse cycle, likely due to impurities building up in the recycled solution.<sup>136</sup> However, the digestibility using the third recycled solution remained significantly higher compared with using fresh solvent or acid. Overall, studies identified two factors that likely contribute to the decrease in enzymatic digestibility observed with recycled solvent. Firstly, residual contaminants, such as degraded hemicellulose and lignin, may remain in the recycled solution despite washing. These contaminants can interfere with the enzymatic breakdown of cellulose in the pretreated bamboo residues.<sup>161</sup> Secondly, the effectiveness of the solvent itself in removing these components may diminish as it is reused.<sup>149</sup>

### 5.2. Catalyst recovery

A study investigated converting LCB to HMF and FF using a heterogeneous catalyst (zeolite) in a biphasic solvent. While it explored reusability, conversion potential dropped significantly – from 64.0% to 32.0% after the third cycle – due to humin adsorption.<sup>76</sup> The 10P-Y catalyst performed consistently well over the first three cycles under optimized conditions for producing HMF. During these cycles, the yield of HMF remained stable at around 65.0%, while FF yield stayed low (~8.0%). However, the HMF yield dipped to 55.0% after the third cycle, accompanied by a slight increase in FF yield (10.0%). This process effectively restored the catalyst's activity, allowing it to perform similarly to a fresh catalyst under the same conditions.<sup>107</sup> Another study investigated the reusability of  $\text{SO}_4^{2-}/\text{SnO}_2^{3-}$ -MMT catalyst for converting corncob sugars to FF. Here, xylose conversion stayed consistent over five cycles, and FF yield gradually dropped. Despite a 4.0% decrease by the second cycle, the catalyst maintained a stable recycling capacity, suggesting its potential for heterogeneous cost-effective, and sustainable FF production.<sup>77</sup>

Homogeneous catalysts, such as chloride or acid salts, are widely studied but suffer significant losses during recycling *via* precipitation and drying. For example, only 50.0% of an oxalic acid catalyst may be recovered through crystallization, highlighting greater losses compared to heterogeneous catalysts.<sup>90</sup> Although one study noted a slight decrease in *p*-TsOH catalyst recovery to 91.5% during the fourth recycling cycle, subsequent research showed no negative impact on cellulose con-

version or delignification yield.<sup>46</sup> Spectral analysis confirmed the exceptional purity of recycled FDCA, exceeding 99.0%.<sup>78</sup> Interestingly, recycled FeCl<sub>3</sub> used in FF production was still stable after 5 runs, and the FF production maintained a yield of over 70.0%.<sup>158</sup>

In conclusion, implementing solvent and catalyst recovery strategies has the potential to significantly reduce the economic burden of LCB pretreatment. Furthermore, integrating energy and heat within the process design holds promise for even greater economic feasibility. While adjustments will undoubtedly be needed for large-scale adoption, the successful recovery of these key components paves the way for a more sustainable and cost-effective approach to LCB pretreatment.

## 6. Sustainability assessments of biphasic solvent systems

To establish the true sustainability of bio-based products, a holistic approach encompassing both economic and environmental factors is imperative. TEA evaluates the economic viability of a process, including cost estimation, optimization, and investment decisions.<sup>162</sup> LCA, on the other hand, focuses on environmental impacts, assessing sustainability, process improvement, and regulatory compliance.<sup>163,164</sup> Integrating TEA and LCA provides a comprehensive evaluation, balancing economic and environmental considerations.<sup>163,164</sup> This approach fosters sustainable development and informed decision-making, ensuring economic benefits do not come at the expense of environmental health.<sup>163,165</sup>

A notable gap in the research on biphasic systems of various bio-based products is the scarcity of integrated LCA and TEA studies. Only a limited number of such studies have been conducted to date. This section provides a review of LCA and TEA studies specifically on biphasic systems for LCB at the industrial level, considering energy balance.

Khounani *et al.* compared pentanol/TsOH (Sc-1) with conventional H<sub>2</sub>SO<sub>4</sub> (Sc-2) for pine chip-based biorefineries. Sc-1 had a 13.0% lower environmental impact due to reduced electricity use and higher product yields (76.0%), but both methods significantly impacted health, ecosystems, and resources, with electricity generation being the main contributor (Fig. 18). The study advocates for sustainable pretreatment methods, greener electricity, and advanced technologies like combined heat and power and carbon capture and storage.<sup>60</sup> This study stands out by conducting a comprehensive LCA, covering midpoint, endpoint, and weighting levels, which offer a more complete understanding of biodiversity, resource, and health impacts.

Another study also investigated the effects of different concentrations of mannitol and metal ion catalysts (FeCl<sub>3</sub>, FeCl<sub>2</sub>, CuCl<sub>2</sub>, AlCl<sub>3</sub>, and MgCl<sub>2</sub>) on the environmental performance of the FF production process.<sup>72</sup> A 5.0% w/w mannitol-aided AlCl<sub>3</sub> combination yielded up to 30.8% and 30.5% reductions in human health and ecosystem damage, respectively. AlCl<sub>3</sub> significantly outperformed other catalysts, reducing overall

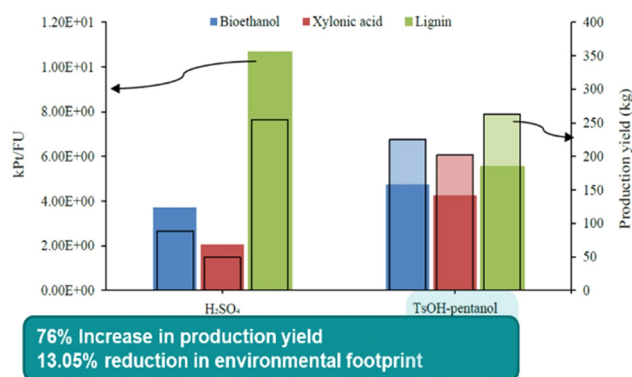


**Fig. 18** Environmental impact comparison of LCB biorefinery in H<sub>2</sub>SO<sub>4</sub> and pentanol/*p*-TsOH systems in processing one tonne of pine chips. Contributions of bioethanol, xylonic acid, and lignin to overall impact are shown at a weighted level.<sup>60</sup> With permission from Elsevier. Copyright©2024. (LN: 5847780889116).

environmental impacts by up to 79.3%. Electricity generation was responsible for the majority of the negative environmental impacts of the FF-producing biorefinery. The substitution of conventional electricity generation with renewable energy sources could significantly reduce the potential environmental damage associated with FF production.<sup>72</sup> Moreover, bamboo residues were converted into bioethanol, polylactic acid, and bio-based wood adhesive using the phenoxyethanol/H<sub>2</sub>SO<sub>4</sub> system. The life-cycle Global Warming Potential (GWP) for bioethanol production ranges from 17.0 to 32.1 grams of CO<sub>2</sub> equivalent per megajoule (gCO<sub>2</sub>e MJ<sup>-1</sup>) when the biphasic system is employed, and from 3.2 to 3.7 kilograms of CO<sub>2</sub> equivalent per kilogram (kgCO<sub>2</sub>e kg<sup>-1</sup>) for polylactic acid production. Without the biphasic system, GWP increases significantly to 135.8 gCO<sub>2</sub>e MJ<sup>-1</sup> for bioethanol and 4.4 kgCO<sub>2</sub>e kg<sup>-1</sup> for polylactic acid. Treating 1 dry ton of bamboo residues achieved a GWP of -174.0 to -66.0 kgCO<sub>2</sub>e for bioethanol and -542.0 to -432.0 kgCO<sub>2</sub>e for polylactic acid, outperforming conventional landfilling, highlighting bamboo residues' potential in promoting a circular bioeconomy and reducing environmental impact.<sup>166</sup>

Similar to LCA, limited information exists on the economic feasibility of biphasic systems. The TEA on producing FF, cellulose pulp, and lignin from switchgrass using water: MIBK system was investigated.<sup>167</sup> The results are promising, with a minimum selling price (MSP) of \$625.0 per ton for FF, approximately 37.0% lower than the current market price. This was based on a 84.0% FF yield and a 95.0% ethanol yield from cellulose pulp, demonstrating a significant economic advantage over other processes designed for the co-production of FF and ethanol.<sup>167</sup> The two-stage process for FF production from birch hydrolysate *via* autohydrolysis, with an MSP of \$1620.0 per ton was developed. Based on the study, the cost reduction in the MIBK process was attributed to the production of multiple market-driven products, including FF, technical lignin, and bioethanol, facilitated by efficient fractionation of switchgrass into three streams for further valorization.<sup>168</sup> A comparative

analysis of the organosolv and biphasic system (called Organocat) demonstrates the process requires a total investment of \$34.4 million, exceeding the Organosolv process by 10.0%. Higher costs stem from pressure vessels and tanks due to an additional crystallizer and larger reactor. Major equipment costs include \$12.5 million for heat exchangers, \$7.7 million for compressors/pumps, and \$9.7 million for washing/drying. Despite higher initial costs, annualized capital, and energy costs are similar to organosolv. Raw material costs (\$7.9 million) account for 51.0% of total costs, with oxalic acid losses increasing expenses. However, higher lignin revenue (\$6.8 million vs. \$3.9 million) leads to \$19.4 million in annual revenue and \$2.4 million in after-tax earnings. This results in a favorable payback period of 3.7 years and ROI of 6.9% showing the superiority (Fig. 20).

Madadi *et al.* recently conducted a comprehensive mass and energy balance analysis on the pentanol/*p*-TsOH system using 1 kg of poplar biomass (Fig. 19). The biorefinery process yielded 232.0 g of native-like lignin, 202.0 g of xylonic acid, and 225.0 g of bioethanol. Notably, pentanol and *p*-TsOH were recycled multiple times from the biphasic fractions, enhancing

the process's economic viability for industrial applications. Milling and distillation emerged as the most energy-intensive stages, consuming 1.9 MJ, while the pretreatment process required the least energy at 0.13 MJ. Remarkably, the biorefinery process achieved a net positive energy gain of 3.6 MJ with an energy ratio of 1.7, significantly outperforming other reported pretreatment methods. The net energy gain of this process is 1.0 to 3.2 times higher than other pretreatments, underscoring the potential of the pentanol/*p*-TsOH system as an efficient fractionation method for converting LCB into valuable bioproducts.<sup>118</sup> According to Khounani *et al.*'s LCA, the pentanol/*p*-TsOH system requires substantial inputs—6.5 L of pentanol and 1 kg of *p*-TsOH—to produce modest quantities of native-like lignin, bioethanol, xylonic acid, and other sugars (0.03 kg, 0.3 L, 0.2 kg, and 0.2 kg, respectively). A mass balance cost analysis, considering global prices in China, reveals a total input cost of \$33.5 per kg of poplar biomass, offset by \$11.7 in product revenue per solvent/catalyst cycle. Despite the ability to recycle the solvent and catalyst four to five times without performance loss, resulting in a net cost of \$13.3 per kg of poplar biomass, this pretreatment system still demonstrates a 13.0% reduction in environmental footprint compared with other approaches.<sup>60</sup> These findings suggest that while the pentanol/*p*-TsOH system shows promise for industrial application due to its environmental benefits, further optimization is necessary to enhance economic viability.

A study investigating the biphasic pretreatment of *Acacia confusa* wood chips using the pentanol/H<sub>2</sub>SO<sub>4</sub> system demonstrated impressive results in producing bioethanol and reactive lignin. The process achieved a net positive energy yield of 1.07 MJ kg<sup>-1</sup> and a 50.3% carbon recovery in the product stream. These outcomes significantly surpassed those of the H<sub>2</sub>SO<sub>4</sub> pretreatment, which had a 17.1% carbon recovery, and the ethanosolv method, which achieved a 49.6% carbon recovery. Moreover, the overall energy balance for the biphasic process showed a net positive energy output of 1.1 MJ kg<sup>-1</sup>, far outperforming the H<sub>2</sub>SO<sub>4</sub> pretreatment's -0.16 MJ kg<sup>-1</sup> and the ethanosolv approach's -1.6 MJ kg<sup>-1</sup>.<sup>41</sup>

Despite some TEAs indicating the profitability of biphasic solvent systems, their scalability remains unpredictable. Consistent performance in terms of product quantity and quality may not be guaranteed during the scale-up process, potentially affecting revenue.<sup>167,169</sup> Another critical factor is solvent loss during solvent recovery, which can significantly impact production costs. Previous studies have reported an 11.0% and 4.6% loss of pentanol and MIBK during the recovery step.<sup>41,106</sup> Examining solvent loss pathways and developing strategies to minimize these losses is crucial for improving the economic viability of this system.<sup>42</sup>

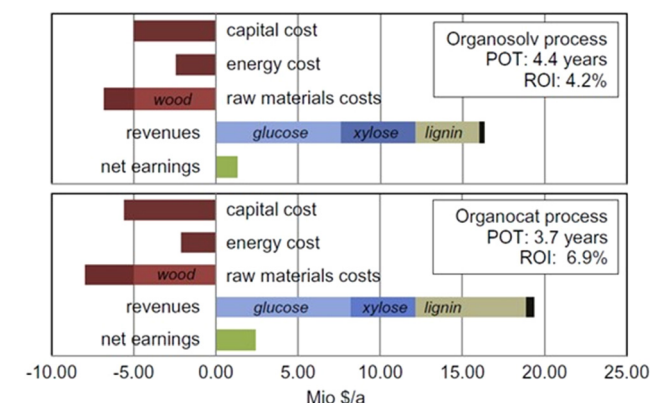


**Fig. 19** This visual compares the yearly expenses, income, and profit for organosolv and Organocat processes. The income is broken down to show the earnings from each product. The portion of the income generated from burning leftover material instead of fossil fuel is shown as a black section in the income bar.<sup>57</sup> With permission from Elsevier. Copyright©2024. (ON: 501926162).

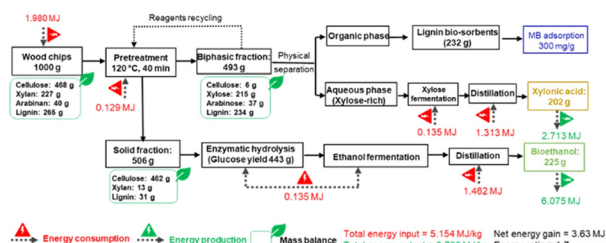


**Fig. 20** The mass and energy balance of proposed biorefinery routes (lignin, xylonic acid, and ethanol) based on 1 kg poplar biomass and pentanol/*p*-TsOH system.<sup>118</sup> With permission from Elsevier. Copyright©2024. (LN: 5847790304827).

## 7. Challenges and future directions

The search for efficient pretreatment methods of LCB fractionation is paramount, with biphasic systems emerging as a particularly promising approach. Biphasic systems offer the

potential to effectively segregate cellulose, hemicellulose, and lignin, each of which is valuable for producing biochemicals and biofuels. However, optimizing the pretreatment process is challenging due to the myriad factors influencing fractionation, including the choice of solvent, catalyst, time, temperature, solid loading, and component ratios. This optimization process is often time-consuming, costly, and susceptible to human and experimental errors. While researchers worldwide are incrementally advancing knowledge about biphasic systems, identifying the optimal conditions remains a complex and lengthy endeavor. A critical challenge lies in predicting laboratory outcomes for LCB pretreatment and biochemical research, which is essential for process optimization and cost reduction. Traditional methods such as statistical modeling, Design of Experiments, and knowledge-based systems, though valuable, are limited by their dependence on extensive past data, expert input, or comprehensive literature reviews. These methods can be cumbersome and may fail to capture the intricate interplay of variables in complex systems. To address these limitations, future research should focus on comprehensive data collection and advanced modeling techniques. Key parameters to analyze include substrate characteristics (cellulose, hemicellulose, lignin, and ash content), solvent properties (acidity, viscosity, polarity, Relative Energy Density, boiling point), catalyst specifications (type, loading, particle size, surface area), and operational conditions (temperature, pressure, residence time, rotational speed, biomass loading). By coupling these data with output metrics such as sugar yields, inhibitor concentrations, and process efficiency, machine learning models can be developed to systematically evaluate and optimize pretreatment performance.

In addition to pretreatment optimization, enhancing enzymatic hydrolysis is crucial for improving overall biomass conversion efficiency. Current studies are limited to solid loadings of 2.0–13.0%, with a notable lack of research on high solid loadings (>15%). Achieving industrial-scale glucose concentrations requires increasing solid loading to 30.0–40.0%, but this introduces mass transfer challenges. Combining fed-batch processes, where fresh substrate is continuously added to the fermentation broth, with machine learning could address these challenges. Machine learning can optimize the feeding process and enzyme addition, potentially unlocking previously inaccessible conditions and enhancing biphasic solvent system technology.

This study underscores the potential of biphasic systems for producing high-quality lignin fractions. However, there is a significant research gap in exploring the utilization of isolated lignin in various applications. Future research could focus on native lignin production for diverse industrial uses or on developing valuable lignin monomers and biochemicals. Additionally, optimizing the biphasic systems process to target specific xylose-based biochemicals such as xylonic acid, levulinic acid,  $\gamma$ -valerolactone, HMF, FF, succinic acid, and glutamic acid could substantially boost the yield of biofuels and advanced materials. Xylonic acid, in particular, stands out with its broad range of applications, from cement additives

and plasticizers to metal chelators and green solvents, and as a precursor for valuable chemicals like ethylene glycol and glycolic acid. This review also highlights a critical gap in LCA and TEA studies on biphasic systems. Future research must evaluate the economic viability and environmental impact of these systems for large-scale industrial implementation. This includes addressing challenges such as waste management during pretreatment, solvent recycling, and minimizing resource consumption and environmental impact across the entire life cycle. Developing a sustainable biomass resource recycling model, supported by computational tools, will be essential for promoting the sustainable use of resources and advancing the commercialization of biphasic systems.

## 8. Conclusion

Biphasic systems represent a substantial advancement in LCB fractionation, providing a robust and effective method for separating its main components. The reusability of solvents and catalysts in these systems significantly enhances both economic and environmental viability, positioning it as a highly attractive option for industrial applications. Our analysis indicates that among the various biphasic systems employed, the alcohol-based pretreatment, particularly the pentanol/*p*-TsOH system, excels in preserving cellulose integrity and maximizing the extraction of xylan and lignin. The lignin recovered from biphasic systems is notable for its high  $\beta$ -O-4 content, purity, and low molecular weight, making it ideal for downstream applications such as lignin nanoparticles and advanced materials. Additionally, the xylose and cellulose preserved during the process have significant potential for producing valuable chemicals and biochemicals, including xylonic acid and bioethanol. Sustainability assessments further underscore the advantages of biphasic systems, demonstrating a potential reduction in environmental footprint compared with traditional methods while enhancing economic feasibility. These findings highlight the promise of biphasic systems in advancing sustainable and efficient biorefinery processes.

## Author contributions

Maryam Saleknezhad: Methodology, Formal analysis, Data curation, Software, Writing – original draft. Meysam Madadi: Project administration, Supervision, Conceptualization, Validation, Investigation, Writing – review & editing. Salauddin Al Azad: Formal analysis, Software. Vijai Kumar Gupta: Validation, Supervision, Writing – review & editing.

## Data availability

The data supporting this article have been included as part of the ESI.†

## Conflicts of interest

The authors declare that they have no known competing financial interests or personal relationships that could have appeared to influence the work reported in this paper.

## Acknowledgements

This work was supported by the National Natural Science Foundation of China (22350410382).

## References

- M. H. Naveed, M. N. A. Khan, M. Mukarram, S. R. Naqvi, A. Abdullah, Z. U. Haq, H. Ullah and H. Al Mohamadi, *Renewable Sustainable Energy Rev.*, 2024, **189**, 113906.
- Z. Zhou, D. Liu and X. Zhao, *Renewable Sustainable Energy Rev.*, 2021, **146**, 111169.
- G. Velvizhi, C. Goswami, N. P. Shetti, E. Ahmad, K. Kishore Pant and T. M. Aminabhavi, *Fuel*, 2022, **313**, 122678.
- S. M. Asaad, M. Tawalbeh and A. Al-Othman, *Int. J. Thermofluids.*, 2024, **21**, 100551.
- H. Shahbeik, H. Kazemi Shariat Panahi, M. Dehghani, G. J. Guillemain, A. Fallahi, H. Hosseinzadeh-Bandbafha, H. Amiri, M. Rehan, D. Raikwar, H. Latine, B. Pandalone, B. Khoshnevisan, C. Sonne, L. Vaccaro, A. S. Nizami, V. K. Gupta, S. S. Lam, J. Pan, R. Luque, B. Sels, W. Peng, M. Tabatabaei and M. Aghbashlo, *Renewable Sustainable Energy Rev.*, 2024, **189**, 113976.
- R. C. Rial, *Renewable Sustainable Energy Rev.*, 2024, **196**, 114369.
- T. vom Stein, P. M. Grande, H. Kayser, F. Sibilla, W. Leitner and P. Domínguez de María, *Green Chem.*, 2011, **13**, 1772–1777.
- A. Ghosh, R. C. Brown and X. Bai, *Green Chem.*, 2016, **18**(4), 1023–1031.
- S. Sikiru, K. J. Abioye, H. B. Adedayo, S. Y. Adebukola, H. Soleimani and M. Anar, *Renewable Sustainable Energy Rev.*, 2024, **200**, 114535.
- K. Karimi, M. Shafiei and R. Kumar, Progress in Physical and Chemical Pretreatment of Lignocellulosic Biomass, in *Biofuel Technologies*, eds. V. Gupta and M. Tuohy, Springer, Berlin, Heidelberg, 2013, ch. 3, pp. 53–96.
- R. Li, Y. Zheng, X. Zhao, Q. Yong, X. Meng, A. Ragauskas and C. Huang, *Green Chem.*, 2023, **25**, 2505–2523.
- L. Xu, S. J. Zhang, C. Zhong, B. Z. Li and Y. J. Yuan, *Ind. Eng. Chem. Res.*, 2020, **59**(39), 16923–16938.
- F. Hu and A. Ragauskas, *Bioenergy Res.*, 2012, **5**, 1043–1066.
- A. R. Mankar, A. Pandey, A. Modak and K. K. Pant, *Bioresour. Technol.*, 2021, **334**, 125235.
- Y. Lv, Y. Zhang and Y. Xu, *Biomass Bioenergy*, 2024, **183**, 107133.
- J. He, C. Huang, C. Lai, C. Huang, M. Li, Y. Pu, A. J. Ragauskas and Q. Yong, *Ind. Crops Prod.*, 2020, **146**, 112205.
- A. Coz, T. Llano, E. Cifrián, J. Viguri, E. Maican and H. Sixta, *Materials*, 2016, **9**(7), 574.
- S. P. Bansod, K. Makwana, P. K. Sarangi and J. K. Parikh, *Sustainable Chem. Pharm.*, 2024, **39**, 101514.
- M. Joshi and S. Manjare, *Environ. Sci. Pollut. Res.*, 2024, **31**, 48928–48954.
- I. Alawad and H. Ibrahim, *Biomass Convers. Biorefin.*, 2024, **14**, 6155–6183.
- M. Sheraz, L. Cao, S. Zhao, H. Gao, P. Dansawad, C. Xue, Y. Li and W. Li, *Arab. J. Sci. Eng.*, 2025, **50**, 3717–3736.
- L. G. Nair, K. Agrawal and P. Verma, *Bioresour. Bioprocess.*, 2023, **10**, 50.
- S. C. Rabelo, P. Y. S. Nakasu, E. Scopel, M. F. Araújo, L. H. Cardoso and A. C. da Costa, *Bioresour. Technol.*, 2023, **369**, 128331.
- Y. Kawamata, T. Yoshikawa, Y. Koyama, H. Ishimaru, S. Ohtsuki, E. Fumoto, S. Sato, Y. Nakasaka and T. Masuda, *Ind. Crops Prod.*, 2021, **159**, 113078.
- D. W. K. Chin, S. Lim, Y. L. Pang, C. H. Lim, S. H. Shuit, K. M. Lee and C. T. Chong, *Sustainability*, 2021, **13**, 6757.
- A. A. Vaidya, K. D. Murton, D. A. Smith and G. Dedual, *Biomass Convers. Biorefin.*, 2022, **12**, 5427–5442.
- C. Sun, G. Song, Z. Pan, M. Tu, M. Kharaziha, X. Zhang, P. L. Show and F. Sun, *Bioresour. Technol.*, 2023, **368**, 128356.
- D. S. Zijlstra, C. W. Lahive, C. A. Analbers, M. B. Figueirêdo, Z. Wang, C. S. Lancefield and P. J. Deuss, *ACS Sustainable Chem. Eng.*, 2020, **8**, 5119–5131.
- P. Lenihan, A. Orozco, E. O'Neill, M. N. M. Ahmad, D. W. Rooney and G. M. Walker, *Chem. Eng. J.*, 2010, **156**, 395–403.
- A. Esteghlalian, A. G. Hashimoto, J. J. Fenske and M. H. Penner, *Modeling and Optimization of the Dilute-Sulfuric-Acid Pretreatment of Corn Stover, Poplar and Switchgrass*, 1997, vol. 59.
- J. Shen and C. E. Wyman, *Bioresour. Technol.*, 2011, **102**, 9111–9120.
- A. Lorenci Woiciechowski, C. J. Dalmas Neto, L. Porto de Souza Vandenberghe, D. P. de Carvalho Neto, A. C. Novak Sydney, L. A. J. Letti, S. G. Karp, L. A. Zevallos Torres and C. R. Soccol, *Bioresour. Technol.*, 2020, **304**, 122848.
- S. Shi, W. Guan, L. Kang and Y. Y. Lee, *Ind. Eng. Chem. Res.*, 2017, **56**, 10990–10997.
- X. Li, Y. Shi, W. Kong, J. Wei, W. Song and S. Wang, *Energy Rep.*, 2022, **8**, 696–709.
- C. Toquero and S. Bolado, *Bioresour. Technol.*, 2014, **157**, 68–76.
- H. Amiri and K. Karimi, *Ind. Eng. Chem. Res.*, 2013, **52**, 11494–11501.
- G. Wan, Q. Zhang, M. Li, Z. Jia, C. Guo, B. Luo, S. Wang and D. Min, *J. Agric. Food Chem.*, 2019, **67**, 10116–10125.
- A. W. Bhutto, K. Qureshi, K. Harijan, R. Abro, T. Abbas, A. A. Bazmi, S. Karim and G. Yu, *Energy*, 2017, **122**, 724–745.
- T. Cai, C. Liu, J. Jiang, X. Meng, A. J. Ragauskas and K. Wang, *Trends Chem.*, 2024, **6**, 219–233.

- 40 C. J. Zimmermann, N. V. Bollar and S. G. Wettstein, *Biomass Bioenergy*, 2018, **118**, 163–171.
- 41 M. K. Islam, S. Rehman, J. Guan, C. Y. Lau, H. Y. Tse, C. S. Yeung and S. Y. Leu, *Appl. Energy*, 2021, **303**, 117653.
- 42 B. Gao, C. Sun, T. Yang, Q. Wen, S. You, Q. Yang, Z. Yang, H. Cheng, Y. Wang, H. Zhou and Z. Chen, Elsevier B.V., 2023, preprint, DOI: [10.1016/j.indcrop.2023.117036](https://doi.org/10.1016/j.indcrop.2023.117036).
- 43 M. Madadi, Zahoor, G. Song, K. Karimi, D. Zhu, M. Elsayed, F. Sun and A. Abomohra, *Bioresour. Technol.*, 2022, **359**, 127503.
- 44 M. Madadi, M. Elsayed, F. Sun, J. Wang, K. Karimi, G. Song, M. Tabatabaei and M. Aghbashlo, *Bioresour. Technol.*, 2023, **371**, 128591.
- 45 M. Madadi, M. M. A. Bakr, G. Song, C. Sun, F. Sun, Z. Hao, Zahoor and A. Abomohra, *J. Cleaner Prod.*, 2022, **366**, 132817.
- 46 M. Madadi, M. Elsayed, G. Song, R. Kumar, M. Mahmoud-Aly, B. Basak, B. H. Jeon and F. Sun, *Chem. Eng. J.*, 2023, **465**, 142881.
- 47 E. Viola, F. Zimbardi, M. Morgana, N. Cerone, V. Valerio and A. Romanelli, *Processes*, 2021, **9**, 2051.
- 48 M. Galbe and O. Wallberg, *Biotechnol. Biofuels*, 2019, **12**(1), 294.
- 49 I. Dávila and J. Labidi, *Curr. Opin. Green Sustainable Chem.*, 2021, **28**, 100435.
- 50 S. Sun, X. Cao, H. Li, X. Chen, J. Tang and S. Sun, *Energy Convers. Manage.*, 2018, **173**, 539–544.
- 51 H. Guo, Y. Chang and D. J. Lee, *Bioresour. Technol.*, 2018, **252**, 198–215.
- 52 J. E. Romo, N. V. Bollar, C. J. Zimmermann and S. G. Wettstein, *ChemCatChem*, 2018, **10**(21), 4805–4816.
- 53 F. Trimble and A. P. Dunlop, *Ind. Eng. Chem., Anal. Ed.*, 1940, **12**(12), 721–722.
- 54 Y. Román-Leshkov, J. N. Chheda and J. A. Dumesic, *Science*, 2006, **312**, 1933–1937.
- 55 R. Weingarten, A. Rodriguez-Beuerman, F. Cao, J. S. Luterbacher, D. M. Alonso, J. A. Dumesic and G. W. Huber, *ChemCatChem*, 2014, **6**, 2229–2234.
- 56 H. Liu, H. Hu, M. S. Jahan and Y. Ni, *Bioresour. Technol.*, 2013, **131**, 315–320.
- 57 J. Viell, A. Harwardt, J. Seiler and W. Marquardt, *Bioresour. Technol.*, 2013, **150**, 89–97.
- 58 G. Calvaruso, M. T. Clough and R. Rinaldi, *Green Chem.*, 2017, **19**, 2803–2811.
- 59 X. Xie, M. Madadi, S. Al Azad, Y. Qiao, M. Elsayed, M. Aghbashlo and M. Tabatabaei, *Fuel*, 2024, **363**, 130890.
- 60 Z. Khounani, N. N. Abdul Razak, H. Hosseinzadeh-Bandbafha, M. Madadi, F. Sun, P. Mohammadi, T. M. I. Mahlia, M. Aghbashlo and M. Tabatabaei, *Environ. Res.*, 2024, **248**, 118286.
- 61 Q. Xin, K. Pfeiffer, J. M. Prausnitz, D. S. Clark and H. W. Blanch, *Biotechnol. Bioeng.*, 2012, **109**, 346–352.
- 62 L. Shuai and J. Luterbacher, *ChemSusChem*, 2016, **9**(2), 133–155.
- 63 S. Rivas, L. López, C. Vila and J. C. Parajó, *Bioresour. Technol.*, 2021, **342**, 125967.
- 64 P. P. Upare, R. E. Clarence, H. Shin and B. G. Park, *Processes*, 2023, **11**(10), 2912.
- 65 M. Madadi, Zahoor, S. W. A. Shah, C. Sun, W. Wang, S. S. Ali, A. Khan, M. Arif and D. Zhu, *Bioresour. Technol.*, 2022, **365**, 128171.
- 66 Q. Zhang, X. Tan, W. Wang, Q. Yu, Q. Wang, C. Miao, Y. Guo, X. Zhuang and Z. Yuan, *ACS Sustainable Chem. Eng.*, 2019, **7**, 8678–8686.
- 67 C. G. Yoo, S. Zhang and X. Pan, *RSC Adv.*, 2017, **7**, 300–308.
- 68 S. Gundekari and S. K. Karmee, *Molecules*, 2024, **29**(1), 242.
- 69 S. Xu, D. Pan, Y. Wu, X. Song, L. Gao, W. Li, L. Das and G. Xiao, *Fuel Process. Technol.*, 2018, **175**, 90–96.
- 70 M. Fernández-Bautista, S. Martínez-Gómez, S. Rivas, J. L. Alonso and J. C. Parajó, *Int. J. Mol. Sci.*, 2023, **24**(15), 12404.
- 71 C. Zhang, C. Y. Ma, L. H. Xu, Y. Y. Wu and J. long Wen, *Int. J. Biol. Macromol.*, 2021, **183**, 1362–1370.
- 72 Z. Khounani, N. N. Abdul Razak, H. Hosseinzadeh-Bandbafha, M. Madadi, F. Sun, I. M. R. Fattah, K. Karimi, V. K. Gupta, M. Aghbashlo and M. Tabatabaei, *Ind. Crops Prod.*, 2023, **203**, 117230.
- 73 F. Yang, Q. Liu, X. Bai and Y. Du, *Bioresour. Technol.*, 2011, **102**, 3424–3429.
- 74 W. Lv, Z. Si, Z. Tian, C. Wang, Q. Zhang, Y. Xu, T. Wang and L. Ma, *ACS Sustainable Chem. Eng.*, 2017, **5**, 2981–2993.
- 75 Z. Xie, B. Chen, H. Wu, M. Liu, H. Liu, J. Zhang, G. Yang and B. Han, *Green Chem.*, 2019, **21**, 606–613.
- 76 O. Ojelabi, S. Yousatit, U. Rashid and C. Ngamcharussrivichai, *Catalysts*, 2023, **13**, 982.
- 77 Q. Qing, Q. Guo, L. Zhou, Y. Wan, Y. Xu, H. Ji, X. Gao and Y. Zhang, *Bioresour. Technol.*, 2017, **226**, 247–254.
- 78 D. Weidener, H. Klose, W. Leitner, U. Schurr, B. Usadel, P. D. de Maria and P. M. Grande, *ChemSusChem*, 2018, **11**, 2051–2056.
- 79 Q. Zhan, Q. Lin, Y. Wu, Y. Liu, X. Wang and J. Ren, *Bioresour. Technol.*, 2023, **376**, 128887.
- 80 K. Dussan, B. Girisuta, M. Lopes, J. J. Leahy and M. H. B. Hayes, *ChemSusChem*, 2016, **9**, 492–504.
- 81 Z. Jiang, V. L. Budarin, J. Fan, J. Remón, T. Li, C. Hu and J. H. Clark, *ACS Sustainable Chem. Eng.*, 2018, **6**, 4098–4104.
- 82 B. Xue, Y. Yang, M. Zhu, Y. Sun and X. Li, *Bioresour. Technol.*, 2018, **270**, 55–61.
- 83 International Chemical Safety Cards (ICSCs).
- 84 C. M. Hansen, *Hansen solubility parameters: a user's handbook*, CRC Press, 2000.
- 85 W. Z. Yin, S. L. Zou, L. P. Xiao and R. C. Sun, *Chem. Eng. Sci.*, 2024, **288**, 119828.
- 86 X. K. Li, Z. Fang, J. Luo and T. C. Su, *ACS Sustainable Chem. Eng.*, 2016, **4**, 5804–5813.
- 87 S. X. Li, M. F. Li, J. Bian, S. N. Sun, F. Peng and Z. M. Xue, *Bioresour. Technol.*, 2017, **243**, 1105–1111.

- 88 P. M. Grande, D. Weidener, S. Dietrich, M. Dama, M. Bellof, R. Maas, M. Pauly, W. Leitner, H. Klose and P. Domínguez De Mariá, *ACS Omega*, 2019, **4**, 14451–14457.
- 89 P. M. Grande, J. Viell, N. Theyssen, W. Marquardt, P. Domínguez De María and W. Leitner, *Green Chem.*, 2015, **17**, 3533–3539.
- 90 A. Morone, R. A. Pandey and T. Chakrabarti, *Ind. Crops Prod.*, 2017, **99**, 7–18.
- 91 H. Teramura, K. Sasaki, T. Oshima, H. Kawaguchi, C. Ogino, T. Sazuka and A. Kondo, *Bioresour. Technol.*, 2018, **252**, 157–164.
- 92 X. K. Li, Z. Fang, J. Luo and T. C. Su, *ACS Sustainable Chem. Eng.*, 2016, **4**, 5804–5813.
- 93 I. Dávila, E. Diaz and J. Labidi, *Bioresour. Technol.*, 2021, **336**, 125311.
- 94 S. Sun, X. Cao, H. Li, Y. Zhu, Y. Li, W. Jiang, Y. Wang and S. Sun, *Polymers*, 2020, **12**, 557.
- 95 Z. Wang, S. Xia, X. Wang, Y. Fan, K. Zhao, S. Wang, Z. Zhao and A. Zheng, *Renewable Sustainable Energy Rev.*, 2024, **196**, 114332.
- 96 S. Rivas, R. Baldassari, J. C. Parajó and A. M. Raspolli Galletti, *Polymers*, 2023, **15**, 1553.
- 97 H. Amiri, K. Karimi and H. Zilouei, *Bioresour. Technol.*, 2014, **152**, 450–456.
- 98 E. Viola, F. Zimbardi, M. Morgana, N. Cerone, V. Valerio and A. Romanelli, *Processes*, 2021, **9**, 2051.
- 99 P. Luo, X. Feng, S. Liu and Y. Jiang, *Drug Des., Dev. Ther.*, 2024, **18**, 6459–6485.
- 100 A. Karnaouri, G. Asimakopoulou, K. G. Kalogiannis, A. A. Lappas and E. Topakas, *Bioresour. Technol.*, 2021, **341**, 125846.
- 101 H. Teramura, K. Sasaki, T. Oshima, F. Matsuda, M. Okamoto, T. Shirai, H. Kawaguchi, C. Ogino, K. Hirano, T. Sazuka, H. Kitano, J. Kikuchi and A. Kondo, *Biotechnol. Biofuels*, 2016, **9**, 27.
- 102 J. Liu, H. Hu, Z. Gong, G. Yang, R. Li, L. Chen, L. Huang and X. Luo, *Cellulose*, 2019, **26**, 3801–3814.
- 103 Q. Zhang, X. Tan, W. Wang, Q. Yu, X. Chen, C. Miao, Y. Guo, Y. Zhang, X. Zhuang, Y. Sun, X. Kong and Z. Yuan, *ACS Sustainable Chem. Eng.*, 2020, **8**, 7649–7655.
- 104 Y. Zhu, R. Tang, Y. Yu, Z. Yu, K. Wang, Y. Wang, P. Liu and D. Han, *Fermentation*, 2023, **9**, 61.
- 105 Q. Zhang, C. Dai, J. Zhang, X. He, X. Tan, K. Zhang, X. Xu and X. Zhuang, *Int. J. Biol. Macromol.*, 2023, **230**, 123249.
- 106 G. Zeng, Z. Wu, W. Cao, Y. Wang, X. Deng and Y. Zhou, *Nat. Prod. Res.*, 2020, **34**, 1041–1045.
- 107 A. Pande, P. Niphadkar, K. Pandare and V. Bokade, *Energy Fuels*, 2018, **32**, 3783–3791.
- 108 Z. Chen, X. Bai, A. Lusi, W. A. Jacoby and C. Wan, *Bioresour. Technol.*, 2019, **289**, 121708.
- 109 Z. K. Wang, X. J. Shen, J. J. Chen, Y. Q. Jiang, Z. Y. Hu, X. Wang and L. Liu, *Int. J. Biol. Macromol.*, 2018, **117**, 721–726.
- 110 L. Zhang, Y. Tian, Y. Wang and L. Dai, *Chin. Chem. Lett.*, 2021, **32**, 2233–2238.
- 111 P. Nechita, M. Roman and S. M. Năstac, *Polymers*, 2023, **15**, 2088.
- 112 A. K. M. H. Morshed, S. Al Azad, M. A. R. Mia, M. F. Uddin, T. I. Ema, R. B. Yeasin, S. A. Srishti, P. Sarker, R. Y. Aurthi, F. Jamil, N. S. N. Samia, P. Biswas, I. A. Sharmeen, R. Ahmed, M. Siddiquy and S. M. Nurunnahar, *Mol. Diversity*, 2023, **27**, 2651–2672.
- 113 L. Sun, Z. Jiang, B. Yuan, S. Zhi, Y. Zhang, J. Li and A. Wu, *Chem. Eng. Res. Des.*, 2021, **174**, 71–78.
- 114 A. De Santi, S. Monti, G. Barcaro, Z. Zhang, K. Barta and P. J. Deuss, *ACS Sustainable Chem. Eng.*, 2021, **9**, 2388–2399.
- 115 H. Q. Pham, V. Bernales and L. Gagliardi, *J. Chem. Theory Comput.*, 2018, **14**, 1960–1968.
- 116 L. Jiang, G. C. Du, J. P. Wang, Z. X. Wu and H. Y. Li, *Sep. Purif. Technol.*, 2025, **361**, 131673.
- 117 M. Rao, H. Xia, Y. Xu, G. Jiang, Q. Zhang, Y. Yuan and L. Zhang, *Hydrometallurgy*, 2022, **230**, 106385.
- 118 M. Madadi, M. Elsayed, G. Song, M. M. Bakr, Y. Qin, F. Sun and A. Abomohra, *Renewable Sustainable Energy Rev.*, 2023, **185**, 113605.
- 119 A. Laca, A. Laca and M. Díaz, Chapter 8 - Hydrolysis: From cellulose and hemicellulose to simple sugars, in *Second and Third Generation of Feedstocks: The Evolution of Biofuels*, eds. A. Basile and F. Dalena, Elsevier, 2019, ch. 8, pp. 213–240.
- 120 Y. Liao, B. O. de Beeck, K. Thielemans, T. Ennaert, J. Snelders, M. Dusselier, C. M. Courtin and B. F. Sels, *J. Mol. Catal.*, 2020, **487**, 110883.
- 121 J. Zhang, Y. Wang, L. Zhang, R. Zhang, G. Liu and G. Cheng, *Bioresour. Technol.*, 2014, **151**, 402–405.
- 122 S. Park, J. O. Baker, M. E. Himmel, P. A. Parilla and D. K. Johnson, *Biotechnol. Biofuels.*, 2010, **3**, 1–10.
- 123 Q. Schmetz, H. Teramura, K. Morita, T. Oshima, A. Richel, C. Ogino and A. Kondo, *ACS Sustainable Chem. Eng.*, 2019, **7**, 11069–11079.
- 124 X. Zhang, Y. Bai, X. Cao and R. Sun, *Bioresour. Technol.*, 2017, **238**, 1–6.
- 125 S. Sun, S. Sun, X. Cao and R. Sun, *Bioresour. Technol.*, 2016, **199**, 49–58.
- 126 H. D. Phan, T. Yokoyama and Y. Matsumoto, *Org. Biomol. Chem.*, 2012, **10**, 7382–7391.
- 127 P. Hu, Y. Hu, H. Li, L. Li, Z. Xue, D. Wu, J. Zhao, C. Hu and L. Zhu, *Carbohydr. Polym.*, 2023, **309**, 120692.
- 128 B. C. Bussamra, S. Freitas and A. C. da Costa, *Bioresour. Technol.*, 2015, **187**, 173–181.
- 129 L. Hoppert and D. Einfalt, *SN Appl. Sci.*, 2021, **3**, 878.
- 130 C. Álvarez, F. M. Reyes-Sosa and B. Diez, *Microb. Biotechnol.*, 2016, **9**(2), 149–156.
- 131 X. Jiang, R. Zhai and M. Jin, *Bioresour. Technol.*, 2021, **329**, 124911.
- 132 M. G. Resch, J. O. Baker and S. R. Decker, Low Solids Enzymatic Saccharification of Lignocellulosic Biomass, Laboratory Analytical Procedure (LAP), National Renewable Energy Laboratory (NREL), 2015.
- 133 N. I. Wan Azelee, H. I. Mahdi, Y. S. Cheng, N. Nordin, R. M. Illias, R. A. Rahman, S. M. Shaarani, P. Bhatt,

- S. Yadav, S. W. Chang, B. Ravindran and V. Ashokkumar, *Fuel*, 2023, **339**, 126982.
- 134 Z. Chen, Y. Wang, H. Cheng and H. Zhou, *Ind Crops Prod.*, 2022, **187**, 115335.
- 135 K. Yoshida, H. Nanao, Y. Kiyozumi, K. Sato, O. Sato, A. Yamaguchi and M. Shirai, *J. Taiwan Inst. Chem. Eng.*, 2017, **79**, 55–59.
- 136 Y. Zheng, Y. Yu, W. Lin, Y. Jin, Q. Yong and C. Huang, *Bioresour. Technol.*, 2021, **325**, 124691.
- 137 Q. Wang, W. Qi, W. Wang, Y. Zhang, N. Leksawasdi, X. Zhuang, Q. Yu and Z. Yuan, *Renewable Energy*, 2019, 139–146.
- 138 N. Sweygers, D. E. C. Depuydt, A. W. Van Vuure, J. Degreève, G. Potters, R. Dewil and L. Appels, *Chem. Eng. J.*, 2020, **386**, 123957.
- 139 J. S. Luterbacher, D. Martin Alonso and J. A. Dumesic, *Green Chem.*, 2014, **16**, 4816–4838.
- 140 L. Yan, R. Ma, H. Wei, L. Li, B. Zou and Y. Xu, *Bioresour. Technol.*, 2019, **279**, 84–91.
- 141 F. Brienza, D. Cannella, D. Montesdeoca, I. Cybulska and D. P. Debecker, *RSC Sustainability*, 2023, **2**, 37–90.
- 142 A. Lorenci Woiciechowski, C. J. Dalmas Neto, L. Porto de Souza Vandenberghe, D. P. de Carvalho Neto, A. C. Novak Sydney, L. A. J. Letti, S. G. Karp, L. A. Zevallos Torres and C. R. Soccol, *Bioresour. Technol.*, 2020, **304**, 122848.
- 143 A. Mittal, S. K. Black, T. B. Vinzant, M. O'brien, M. P. Tucker, D. K. Johnson and D. K. Johnson, *ACS Sustainable Chem. Eng.*, 2017, **5**(7), 5694–5701.
- 144 L. J. Jönsson and C. Martín, *Bioresour. Technol.*, 2016, **199**, 103–112.
- 145 H. X. Lu, W. Y. Yang, Y. X. Shi, H. Bin Wang, H. Mao, L. Sang and Z. P. Zhao, *Chem. Eng. Sci.*, 2023, **266**, 118256.
- 146 C. Vila, R. Yáñez and J. L. Alonso, *Ind. Crops Prod.*, 2023, **206**, 117581.
- 147 Y. Zheng, X. Zhao, W. Lin, Q. Yong and C. Huang, *Ind. Crops Prod.*, 2023, **199**, 116663.
- 148 Q. Zhang, C. Dai, X. Tan, X. He, K. Zhang, X. Xu and X. Zhuang, *Bioresour. Technol.*, 2023, **369**, 128477.
- 149 Q. Zhang, Y. Deng, X. Tan, W. Wang, Q. Yu, X. Chen, C. Miao, Y. Guo, Y. Zhang, X. Zhuang and Z. Yuan, *Ind. Crops Prod.*, 2020, **145**, 112091.
- 150 Q. Zhang, H. Li, Z. Guo and F. Xu, *Polymers*, 2020, **12**, 378.
- 151 M. López, V. Santos, J. C. Del Río, J. Rencoret and J. C. Parajó, *ACS Sustainable Chem. Eng.*, 2020, **8**, 10115–10124.
- 152 G. Calvaruso, M. T. Clough and R. Rinaldi, *Green Chem.*, 2017, **19**, 2803–2811.
- 153 T. Xiao, M. Hou, X. Guo, X. Cao, C. Li, Q. Zhang, W. Jia, Y. Sun, Y. Guo and H. Shi, *Renewable Sustainable Energy Rev.*, 2024, **192**, 114243.
- 154 W. Schutyser, T. Renders, S. Van Den Bosch, S. F. Koelewijn, G. T. Beckham and B. F. Sels, *Chem. Soc. Rev.*, 2018, **47**, 852–908.
- 155 I. Salapa, C. Katsimpouras, E. Topakas and D. Sidiras, *Biomass Bioenergy*, 2017, **100**, 10–16.
- 156 F. Foltanyi, J. E. Hawkins, I. Panovic, E. J. Bird, T. M. Gloster, C. S. Lancefield and N. J. Westwood, *Biomass Bioenergy*, 2020, **141**, 105680.
- 157 D. Weidener, M. Dama, S. K. Dietrich, B. Ohrem, M. Pauly, W. Leitner, P. Domínguez De María, P. M. Grande and H. Klose, *Biotechnol. Biofuels*, 2020, **13**, 155.
- 158 Q. Zhang, Z. Guo, X. Zeng, B. Ramarao and F. Xu, *Renewable Energy*, 2021, **179**, 351–358.
- 159 J. Cheng, C. Huang, Y. Zhan, X. Liu, J. Wang, C. Huang, G. Fang, A. J. Ragauskas, Z. Xie and X. Meng, *Bioresour. Technol.*, 2023, **387**, 129653.
- 160 J. Liang, K. Wang, C. Huang, T. Cai, C. Liu, J. Ye, W. Tan and J. Jiang, *Ind. Crops Prod.*, 2023, **195**, 116481.
- 161 X. J. Shen, J. L. Wen, Q. Q. Mei, X. Chen, D. Sun, T. Q. Yuan and R. C. Sun, *Green Chem.*, 2019, **21**, 275–283.
- 162 Y. Liu, Y. Lyu, J. Tian, J. Zhao, N. Ye, Y. Zhang and L. Chen, *Renewable Sustainable Energy Rev.*, 2021, **139**, 110716.
- 163 H. Ansarinasab, M. Mehrpooya and M. Sadeghzadeh, *J. Therm. Anal. Calorim.*, 2021, **145**, 1053–1073.
- 164 R. Mahmud, Integration of Techno-Economic Analysis (TEA) and Life Cycle Assessment (LCA) for Sustainable Process Design, PhD thesis, Clemson University, 2022.
- 165 S. Meramo, P. Fantke and S. Sukumara, *Biotechnol. Biofuels Bioprod.*, 2022, **15**(1), 144.
- 166 C. Huang, R. Li, Y. Zheng and K. Lan, *Chem. Eng. J.*, 2024, **489**, 151181.
- 167 G. Zang, A. Shah and C. Wan, *J. Cleaner Prod.*, 2020, **260**, 120837.
- 168 G. Gómez Millán, R. P. Bangalore Ashok, P. Oinas, J. Llorca and H. Sixta, *Biomass Convers. Biorefin.*, 2021, **11**, 2095–2106.
- 169 J. Cristóbal, C. Caldeira, S. Corrado and S. Sala, *Bioresour. Technol.*, 2018, **259**, 244–252.